IDENTIFICATION OF PUTATIVE INTERACTING PROTEINS WITH cTHY28

by

CHRISTOPHER B. STEPHENS

(Under the Direction of Mark Compton)

ABSTRACT

cTHY28 is a highly conserved, nuclear protein that was identified in a screen of cellular proteins that mediate apoptosis in avian lymphocytes. To determine the cellular function of cTHY28, a co-immunoprecipitation assay was developed to identify proteins that interact with cTHY28. Mass spectrometric analysis of co-immunoprecipitated material from DT-40 lymphocytes revealed three putative interacting proteins: nucleolin, DNA topoisomerase I and elongation factor-2. From a functional perspective, nucleolin is associated with pre-rRNA processing, DNA topoisomerase I relaxes supercoiled DNA, and elongation factor-2 is involved in protein translation. Since these proteins have a direct, protein-protein interaction with cTHY28, it is hypothesized that cTHY28 may augment their cellular function.

INDEX WORDS: cTHY28, Nucleolin, DNA Topoisomerase I, Co-Immunoprecipitation, Protein-Protein Interactions

IDENTIFICATION OF PUTATIVE INTERACTING PROTEINS WITH cTHY28

by

CHRISTOPHER B. STEPHENS

B.S.A., The University of Georgia, 2009

A Thesis Submitted to the Graduate Faculty of The University of Georgia in Partial Fulfillment of the Requirements for the Degree

MASTERS OF SCIENCE

ATHENS, GEORGIA

2011

IDENTIFICATION OF PUTATIVE INTERACTING PROTEINS WITH cTHY28

by

CHRISTOPHER B. STEPHENS

Major Professor:	Mark Compton
Committee:	Adam Davis Erica Spackman

Electronic Version Approved:

Maureen Grasso
Dean of the Graduate School
The University of Georgia
December 2011

DEDICATION

For my son Liam, may this research add a little more knowledge to the world that you will one day inherit.

ACKNOWLEDGEMENTS

I would like to thank my family and loved ones for their emotional support throughout the research, as well as the writing of this thesis. I would also like to thank Mark Compton for his time, his patience, and for making this phase of my education most enjoyable.

TABLE OF CONTENTS

LIST OF TABLES

Page

LIST OF FIGURES

Page

CHAPTER 1: INTRODUCTION

cTHY 28

Previous research in our laboratory involved the design of a screening procedure used to identify cellular proteins with internucleosomal cleavage activity that mediates apoptosis in chicken lymphocytes. From this screen, a gene encoding for a 242 amino acid protein was isolated and referred to as chicken Thy28 (cThy28) (1). cTHY28 expression was found to be highest in bursal, thymus, and spleen tissues. Other tissues, including the brain, liver, kidney, muscle, and small intestine showed a reduced level of expression when compared to the lymphoid tissues (1).

cTHY28 was found to be a conserved protein, sharing 90% amino acid similarity with several mammalian homologues (1). One such homologue, murine Thy28 (mThy28), has been cloned, and its genomic organization analyzed. The mThy28 gene like cThy28 (unpublished data) is encoded by eight exons and seven introns (2). In the 5' flanking region, a basal promoter activity and a negative regulator of promoter activity were found, along with a CCAAT box (2). mTHY28 encodes a protein that is comprised of 226 amino acids that shares a high degree of homology (87%) with the 242 amino acid sequence of cTHY28 (2). The expression pattern of the mThy28 gene differed from that of cThy28. The highest levels of expression were detected in the testes, with moderate expression levels found in the spleen, thymus, liver, and kidney (3).

Based upon the amino acid sequence of cTHY28, several putative structural motifs have been identified: kinase phosphorylation sites (Caesin-Kinase II and Protein Kinase C), a N-linked glycosylation site, and a nuclear localization signal (1). It has since been confirmed that

cTHY28 is a phosphoprotein based upon metabolic labeling of cTHY28 in cell culture with ^{32}P-organophosphate, followed by immunoprecipitation and autoradiography (unpublished data). Nuclear localization of two cThy28 homologues, mThy28 and human Thy28 (hThy28) has also been confirmed. Nuclear localized fluorescence was detected when HEK 293T cells were transfected with an mThy28/EGFP construct (3,4). Likewise, HeLa cells were transfected with a hThy28/EGFP construct, and fluorescent nuclear and nucleolar localization were observed (5).

It has been hypothesized that cTHY28 plays a role in the apoptotic process, since it was isolated using a screen to detect apoptosis mediators. Analysis of bursal lymphocytes undergoing apoptosis indicates that cTHY28 is degraded as a function of time; however the role of this proteolysis in the apoptotic process is unknown (1). In other studies cThy28 mRNA expression was found to be down-regulated in two lines of chicken embryos that had been infected with infectious bursal disease virus (IBDV). This viral infection induces apoptosis in chicken embryos and tissue culture cells; however, the specific role of cThy28 down-regulation in the apoptotic process is unknown (6-10). Similarly, induction of apoptosis in Ramos B lymphomas also resulted in a reduction in the expression of mThy28 at both the mRNA and protein levels; however, the role of this reduction in gene expression on the apoptotic process has yet to be identified (3).

Co-Immunoprecipitation

At all levels of cellular function, protein-protein interactions have been detected, and the study of these protein complexes has become an area of intense research interest in cell biology. These protein complexes are involved in the structure of the sub-cellular components, the transport of materials across membranes, chromatin packaging, regulation of gene expression, and the transduction of intracellular and extracellular signals (11). When presented with a

protein of unknown function, analysis of protein-protein interactions with known protein complexes can reveal clues to the functionality of the unknown protein.

The purification of protein complexes has been accomplished by techniques ranging from gel filtration to immunoaffinity chromatography (12). For example, size exclusion chromatography was used to purify a high molecular weight (1,600 kDa) protein complex from *E. coli* spheroplast that included all the enzymes in the glycolytic pathway (13). Similar techniques, such as enzyme gel chromatography and gel filtration equilibrium analysis, have been used to analyze protein-protein interactions between other metabolic enzymes including citrate synthase and pyruvate dehydrogenase, as well as glutamate dehydrogenase and aspartate amino-transferase (12,14).

Oftentimes, physiologically relevant interactions between cellular proteins can only be detected in solutions that mimic intracellular conditions. As such, immobilization of proteins on a chromatographic matrix represents an excellent tool to analyze these protein-protein interactions (12,15). For this type of protein affinity chromatography, relatively large amounts of the purified protein of interest are generated and covalently linked to a column matrix. A crude cellular extract is then prepared and passed over the affinity column. By manipulating the chromatographic buffer conditions, specific interacting proteins avidly bind to the affinity protein matrix while nonspecific interacting proteins pass through the column. Bound interacting proteins are eluted from the affinity matrix using a buffer containing an elevated salt concentration, chaotropic agent, or an altered pH. Eluted proteins are then identified using mass spectrometric analysis. Numerous protein complexes have been analyzed using this technique. For example, actin and microtubule binding proteins, RNA polymerase C-terminal tail-binding proteins, Sir2 and Sir 4-binding proteins, and complexes associated with cell cycle control

proteins have been characterized using this methodology (16-24). Protein affinity chromatography provides two major benefits. First, low concentrations of low affinity interacting proteins can be captured from cell lysates since relatively high concentrations of the purified protein of interest are attached to the chromatographic matrix. Second, the chromatographic conditions can be performed using buffers that differ from the buffers used to generate the cell lysate. This allows the creation of conditions that are ideal for solubilizing proteins in the lysis steps, and the use of physiological buffer conditions for the affinity chromatography stage (15). However, there is a caveat to the use of bacterial expressed proteins to generate the affinity matrix; they lack post-translational modifications that may be necessary for genuine protein-protein interactions. Fortunately, immunoaffinity chromatography provides an approach that has the benefits of protein-protein affinity chromatography, and the ability to specifically isolate multi-protein complexes under native conditions.

Immunoaffinty chromatography, or immunoprecipitation, is a technique that uses specific antibodies to capture target antigens. Antibodies directed against the protein of interest are covalently linked to a column matrix. The matrix, or resin beads, are then incubated with a lysate prepared from tissues or cells grown in cell culture. Similar to protein-protein affinity chromatography, the cell lysate can be prepared using a buffer that has been optimized for cell lysis, while an alternate buffer system can be used that has been optimized for antibody binding. After binding of the antigen to the antibody, the matrix is washed with a buffer that removes non-specifically bound proteins. Specific proteins that are bound to the antibody matrix are captured by using an elution buffer (15). A variation on this method is the co-immunoprecipitation assay, which captures proteins that interact with the target protein that have been “pulled down” using immunoprecipitation techniques.

A major advantage to using co-immunoprecipitation assays is the ability to manipulate several facets of the assay, including: the antibody and antibody resin, the wash conditions and the elution conditions. There are various types of resins employed in this assay procedure including: natural polysaccharides (agarose, cellulose), organic polymers (polyacrylamide, polyacrylate), and inorganic polymers (silica) (25). The natural polysaccharides were some of the first materials used in co-immunoprecipitation assays and are suitable for the broadest range of applications. These stable resins permit the use of buffers that span a broad pH range (pH 3-pH 13). Furthermore, the natural polysaccharides have a hydrophilic surface, which reduces non-specific protein binding to the resin (26). On the other hand, the organic polymers, as compared to natural polysaccharides, offer better stability for high pressure liquid chromatographic applications; however, their hydrophobic surfaces decrease antibody binding efficiency, as well as increases non-specific binding to the resin (27). Although inorganic silica polymers are widely used as a general chromatographic matrix, these matrices are impractical for immunoaffinity chromatography since silica tends to solubalized under mild alkaline pH conditions that are frequently employed in elution buffers (28).

For immunoprecipitation procedures, polyclonal antibodies are oftentimes employed since they bind to multiple epitopes and thereby enhance the capture of the target protein. Generation of polyclonal antibodies involves the purification of the protein, immunization of animals with the protein, and the collection and purification of immunoglobulins directed against the antigen. For this procedure, the target protein can be generated using recombinant DNA techniques and a bacterial protein expression system. Purification of the expressed protein can be facilitated by engineering an epitope tag (six histidines) into the target protein and using

affinity chromatographic techniques (metal chelation chromatography) to purify the expressed protein (29,30).

As an alternative strategy, a fusion protein can be generated that consists of the target protein linked to a molecular tag protein, for example, Green Fluorescent Protein (GFP). Antibodies directed against the molecular tag protein can be used to immunoprecipitate the target protein in a cell line that has been transfected with the fusion protein. Furthermore, use of the GFP molecular tag permits the intracellular localization of the target protein in transfected cells using fluorescent microscopy (31,32). However, a potential disadvantage of this strategy is the possibility that the tag protein could interfere with the cellular function of the target protein or the formation of protein complexes with the target protein (30).

While immunoprecipitation using molecular tags has been successfully adapted to analyze relatively stable protein complexes, analysis of weak or transient protein complexes has been elusive due to their high disassociation constants (K_{diss}) (33,34). Typically, these weak or transient protein complexes are lost during the stringent wash steps used in the immunoprecipitation assay that are designed to remove non-specific protein interactions (35). However, this dilemma can be avoided by chemically cross-linking the cellular proteins prior to the immunoprecipitation procedure (36). Formalin has been shown to have several characteristics that make it an excellent reagent for protein cross-linking. Formalin can readily permeate the cell membrane and cross-link proteins *in situ* that are in close proximity (less than 2 Angstroms). Furthermore, this chemical cross-linking can be reversed (using heat and an anionic detergent) to permit the analysis of the protein subunits in the complex (37-39). Formalin-cross linking, in conjunction with immunoprecipitation assays, has been used to analyze numerous protein complexes, including: transcription factors and components of multimeric chromatin,

analysis of nucleosomal proteins, and the analysis of transcription factors in yeast cells (37,38,40-42). Thus, the addition of formalin-cross linking to immunoprecipitation assays and the use of molecularly tagged proteins allows not only for the isolation of stable protein complexes, it also permits the capture of weak and transient protein complexes as well.

Protein Identification by Mass Spectrometric Analysis

Mass spectrometric analysis is a powerful technique that can be employed to identify small quantities of protein that are present in immunoprecipitated samples. Compared to Edman degradation sequence analysis based technology, mass spectrometry is a more rapid, versatile method that can detect peptide concentrations in the femtomole-attomole range (43). Furthermore, this instrumentation can be adapted for the analysis of single proteins, protein complexes, or entire proteomes (44).

Prior to mass spectrometric analysis, protein samples containing immunoprecipitated products can be subjected to a variety of purification protocols including SDS-PAGE, 2-D gel electrophoresis, as well as liquid chromatographic procedures (45). Separated proteins are then subjected to trypsin digestion. This proteinase generates peptide fragments with a basic amino acid at the C-terminus which are favorable for peptide detection and amino acid sequence analysis (44).

At this point in the analysis, two different mass spectrometric approaches can be employed: peptide mass fingerprinting (PMF) or tandem mass spectrometry (MS/MS). In the first method, PMF, the mass of each tryptic peptide fragment is determined; however, the amino acid sequence of the peptide remains unknown (46). The mass spectra of each tryptic fragment are determined by matrix-assisted laser desorption/ionization time of flight mass spectrometry (MALDI ToF MS). Since the amino acid sequence of the peptide is not generated, this analysis

compares the set of tryptic peptide mass spectra with a database containing proteins that have been digested *in silico* using the same digestion enzyme. Since each protein in the database has a characteristic set of tryptic peptide mass spectra measurements, it can serve as a unique fingerprint to identify unknown protein from a set of experimentally generated peptide fragments.

The PMF technique is a relatively simple procedure that can be performed rapidly and the results are easy to interpret. However, the reference database that is used must contain greater than 80% of the coding sequence of a protein of interest to accurately compare it to the experimentally generated peptides. Furthermore, numerous tryptic peptides must be generated from a protein in order to query the database for accurate protein identification. Thus, smaller proteins (<15 kDa) cannot be identified efficiently, since these proteins will not generate a sufficient number of tryptic peptide fragments that are needed for accurate protein identification.

Tandem mass spectrometry is an alternate procedure that offers most of the benefits of PMF, while exceeding the sensitivity limitations of PMF. MS/MS works by first measuring the mass of the tryptic peptide fragment. Ion-trap mass spectrometers are the instrument of choice for this type of analysis, instead of the MALDI ToF instruments (47). Ion-trap instruments use an electrospray ionization method, in place of the MALDI method, and generate ions from the peptide solution using a high voltage current (2-6 kV) and the mass spectra of these peptides is determined (48). Simultaneously, the peptide ions are subjected to collisions with an inert gas. This protocol cleaves the peptide backbone, generating fragments that differ by one amino acid. These secondary peptide fragments are then measured by mass spectroscopy to generate a new set of signals which correspond in mass to adjacent amino acid residues in the sequence, thus generating a short segment of peptide amino acid sequence (49). The generated peptide

sequence, the entire peptide mass spectra, and the fragment mass spectra can then be queried against a database that, like the database used for PM, contains the *in silico* predicted fragmentation of proteins of interest. Furthermore, each unique peptide that is analyzed can be used to independently identify a protein (50,51). Protein identity can be further corroborated by the presence of multiple peptides that identify the same protein. Thus, fewer tryptic peptides are required to identify a protein using the MS/MS approach, as compared to PMF methodology.

Thus, the purpose of the described studies in this thesis was to develop strategies that would permit the detection of protein-protein interactions with cTHY28. Accordingly, a co-immunoprecipitation assay was developed that employed a cell line that overexpressed the cThy28 gene. Furthermore, a formalin cross-linking technique was used to enhance the detection of interacting proteins, and mass spectrometric analysis was employed to identify putative interacting proteins.

CHAPTER 2: MATERIALS AND METHODS

Reagents

The following reagents were obtained from Sigma Chemical Company (St. Louis, MO): penicillin, streptomycin sulfate, amphotericin B, lysozyme, pepstatin A, aprotinin, Freund's Complete and Incomplete adjuvants, sodium azide (NaN_3), bovine serum albumin (BSA), sodium vandate, leupeptin, bestatin, E-64, ditiothreitol (DTT), ethylenediamine tetracetic acid (EDTA), 4-(2-Aminoethyl) benzenesulfonyl fluoride hydrochloride (AEBSF), deoxycholate, β-mercaptoethanol (BME), bromphenol blue, methanol, polysorbate 20 (Tween 20), goat anti-rabbit IgG alkaline phosphatase conjugate, rabbit anti-chicken IgY alkaline phosphatase conjugate, goat serum, rabbit serum, sodium carbonate (Na_2CO_3), iodoacetamide, trifluoroacetic acid (TFA), guanidine hydrochloride, IGE-PAL, Triton X-100, and ammonium bicarbonate (NH_4HCO_3). The following reagents were obtained from J.T. Baker (Phillipsburg, NJ): sodium chloride (NaCl), formalin, sodium fluoride (NaF), glycerol, gelatin, magnesium chloride ($MgCl_2$), acetic acid, sodium thiosulfate ($Na_2S_2O_3$), silver nitrate ($AgNO_3$), and potassium ferricyanide. The following reagents were obtained from Promega Corporation (Madison, WI): Xho1, BamH1, EcoR1, nitro blue tetrazolium chloride (NBT), 5-bromo-4-chloro-3-indolyl phosphate (BCIP), and trypsin (sequencing grade). The following reagents were obtained from Fisher Scientific (Pittsburgh, PA): newborn calf serum, TRIS, imidazole, P.E.G 8000, sodium dodecyl sulfate (SDS), acetonitrile, Coomassie Blue stain, Amino Link Plus Coupling Resin, and sodium cyanoborohydride. The glycine was obtained from VWR (Radnor, PA).

DT-40 Cell Culture

The DT-40 cell line (ATCC Cell Line CRL-2111) is derived from an avian leukosis-induced bursal lymphoma from a White Leghorn chicken (52). The cells were cultured at 37°C in a humidified, 5% CO_2 atmosphere in RPMI 1640 medium (GIBCO BRL Life Technologies, Grand Island, NY) containing 5% heat-inactivated New Born Calf Serum, 5% heat-inactivated broiler serum, 50 units/ml penicillin G, 50 μg/ml streptomycin sulfate and 10 μg/ml amphotericin B. The cells were plated at a density of $1x10^5$ cells/ml and harvested 3 days later at a density of ~ $1x10^6$ cells/ml.

Generation of DT-40 N4 and DT-40 V11 Cell Lines

To develop a cell line that expressed a cTHY28/EGFP fusion protein, the N-terminal fusion protein vector pEGFP-N3 (ClonTech, Palo Alto, CA) was employed. Briefly, PCR methodology was used to generate a construct that incorporated an EcoR1 restriction site and a Kozak recognition sequence (Forward PCR Primer: 5'-AGA ATT CGC CGC CAT GCC CTG GCC GAG C-3') that flanked the 5' ATG of cThy28 (GenBank Accession Number 34350). At the 3' end of the gene, the TAA stop codon was deleted and a BamH1 restriction site was inserted (Reverse PCR Primer: 5'-GCG GAT CCA TGT GGC TTT TCC TC-3'). This construct was ligated into the EcoR1/BamH1 multicloning site of the pEGFP-N3 expression vector to generate the cThy28/EGFP construct (Figure 1). To generate the DT-40 N4 cell line, this construct was transfected into the DT-40 WT (wild type) cell line by electroporation. Two hundred and fifty microliters of DT-40 cells ($4x10^7$ cells/ml) in RPMI-1640 medium, were placed in a 0.4 cm cuvette at 4°C and electroporated with 25 μg of Xho1 linearized cThy28/EGFP plasmid DNA using a Bio Rad Gene Pulser II electroporation system set at 250 volts and 960 uF. Subsequently, the electroporated cells were cultured in medium containing

800 μg/ml G418 to select for stably transfected cells. To obtain clonal cell lines, the transfected cells were subjected to flow cytometric cell sorting using a Coulter Epic Elite flow cytometer equipped with an aragon laser set an excitatory wavelength of 488 nm and emitted green fluorescence was detected using a 510/540 nm band pass filter. Individual cells were collected in 96 well plates to generate clonal cell lines, including the DT-40 N4 clonal cell line (Figure 2, Panels A and B) used in these experiments. In a similar fashion, the DT-40 V11 cell line (Figure 2, Panels C and D) was generated; however, this cell line was transfected with 25 μg of Xho1 linearized pEGFP-N3 plasmid DNA.

Generation and Purification of EGFP Antibodies

To generate antibodies directed against the EGFP portion of the cTHY28/EGFP fusion protein, a bacterial-expressed GFP protein was employed as an antigen to immunize White Leghorn hens. [The amino acid sequence of the EGFP protein and the GFP protein are similar; however, the EGFP protein has a double amino acid substitution (Phe-64 to Leu and Ser-65 to Thr) to optimize emitted green fluorescence (53)]. The GFP antigen was generated using a pET-28a/GFP construct that was kindly provided by Dr. Henry Tomasiewicz at Emory University. This construct was transformed into *E. coli* BL21 (DE3). The GFP gene product was over-expressed in the bacterial cells by induction with 1 mM IPTG (isopropyl β-D-thiogalactopyranoside) for four hours. Five hundred milliliters of the bacterial cell culture was harvested by centrifugation (8000 x g, 10 minutes at 4° C). The bacterial pellet was lysed in 50 ml of lysis buffer (20 mM Tris pH 7.9, 500 mM NaCl, 5 mM imidazole, 0.1% Triton X-100, 100 μg/ml lysozyme, 1mM pepstatin A, and 10 μg/ml aprotinin). The bacterial lysate was centrifuged at 39,000 x g for 10 minutes at 4°C, and the supernatant fraction was sonicated briefly (1). The GFP protein was isolated from the bacterial lysate using metal chelation

chromatography to affinity purify the expressed construct containing a 6-histidine tag at the amino terminus of the protein. The bacterial lysate was loaded onto a 2 ml His-Bind column (Novagen, Madison, WI) and unbound bacterial proteins were removed from the column using a wash buffer (20 mM Tris pH 7.9, 500 mM NaCl, and 60 mM imidazole). The histidine-tagged GFP protein was eluted from the column and dialyzed against a buffer containing 50 mM Tris pH 7.4 and 150 mM NaCl. The time course of GFP expression in bacterial culture and purification using metal chelation affinity chromatography is shown in Figure 3.

Antibodies directed against GFP were generated in White Leghorn Hens as previously described (1) in accordance with the guidelines of the University's Animal Care and Use Committee. Prior to immunization, eggs from five hens were collected for a two-week period to generate a pool of control pre-immune antibodies. Hens were initially immunized (intramuscular injection into the pectoralis major muscle) with 200 μg of purified GFP solubalized in 500 ul PBS and 500 Freund's Complete Adjuvant. Two weeks later, a booster injection of 200 μg of purified GFP solubalized in 500 ul of PBS and 500 ul of Freund's Incomplete Adjuvant was administered. A similar booster injection was repeated two weeks later. Immune eggs were then collected from one week to six weeks after the last injection to generate a pool of immune antibodies.

Chicken anti-GFP antibodies were then isolated from the eggs using a polyethylene glycol (P.E.G.) purification procedure (54) . Egg yolks were isolated from the egg and washed with H_2O, and diluted 4:1 with lysis buffer (10 mM Tris HCl pH 7.5, 100 mM NaCl). 3.5% (wt/vol) of P.E.G. 8000 was added to the mixture and centrifuged at 14,000 x g for 10 minutes at 4°C. The supernatant fraction was then removed and filtered through three layers of cheesecloth. 9.0% (wt/vol) P.E.G. 8000 was added to this supernatant fraction and the centrifugation step was

repeated. The supernatant fraction was discarded and the immunoglobulin-enriched pellet was solubalized in lysis buffer. The P.E.G. precipitation procedures and centrifugation steps were repeated. The resulting 9.0% P.E.G. precipitate was solubalized in lysis buffer containing 0.02% NaN_3 and stored at 4°C. Using this purification technique, 50-100 mg of enriched IgY protein was generated from each egg.

To further purify the P.E.G. precipitated chicken anti-GFP antibodies, anionic exchange column chromatography using a DEAE Sepharose matrix was employed (1.5 cm x 6.0 cm). Approximately 50-100 mg of the P.E.G. purified antibodies were dialyzed against the column-loading buffer (10mM Tris pH 8.5) and loaded onto the column. Contaminating yolk proteins were eluted from the column using a solution of 50mM NaCl. IgY antibodies were then eluted from the column using a solution of 250 mM NaCl (Figure 4, Panel A). The resulting column fractions were analyzed using a 12.5% SDS-PAGE and Coomassie Blue stain (Figure 4, Panel B). This analysis showed that a non-IgY contaminating yolk protein was present in the 50mM NaCl column fraction, whereas the 250 mM NaCl fraction was enriched in IgY antibodies (~98% pure as determined by scanning densitometric analysis). Thus, each egg contained ~35 mg of purified IgY.

Covalent Linkage of Antibodies to AminoLink Plus Coupling Resin

For the co-immunoprecipitation assay, chicken anti-GFP antibodies or rabbit anti-cTHY28 antibodies were covalently linked to Amino Link Plus Coupling Resin according to the manufacturer's recommendations (Thermo Fisher Scientific, Rockford, IL). Briefly, for each 1.0 ml bed volume of coupling resin, 5 mg of antibodies (solubalized in 1.0 ml of PBS, pH 7.2) was incubated with the coupling resin overnight at 4°C in the presence of 50 mM sodium cyanoborohydride. After the incubation step, an aliquot of the solution was obtained to calculate

the coupling efficiency. The resin was washed three times with the coupling buffer by low speed centrifugation (290 x g, for 2 minutes, at room temperature). To quench unreacted sites on the coupling resin, 1.0 ml of 1 M Tris pH 7.4 was added to the resin and incubated at room temperature for 30 minutes in the presence of 50 mM sodium cyanoborohydride. The resin was washed three times with 1 M NaCl using the same centrifugation steps as described above. The antibody resin was then stored at 4°C in PBS (pH 7.4) containing 0.05% NaN_3.

Formalin Cross-Linking of DT-40 Cellular Proteins

Formalin was used as a reagent to cross-link interacting DT-40 cellular proteins that bind to cTHY28. Subsequently, the antibody affinity matrix was used to capture the cTHY28/Interacting Protein complex. DT-40 cells were grown to a cell density of ~1.6 x 10^6 cells/ml and incubated with 0.25% formalin for 10 minutes at 37°C. The cross-linking step was quenched by the addition of 125 mM glycine and incubation for 5 minutes at 37°C. The cross-linked cells were harvested by centrifugation (290 x g, for 15 minutes, at 4°C) and the cell pellet was washed two times with PBS (pH 7.4). The washed cell pellet was stored at -80°C.

Co-Immunoprecipitation Assay

Following the formalin cross-linking procedure, DT-40 cell cellular proteins were prepared for use in the Co-Immunoprecipitation Assay. The frozen cells were lysed by brief sonication using an IGE-PAL non-ionic detergent lysis buffer containing proteinase and phosphatase inhibitors (1:1 ratio, cell pellet volume/lysis buffer volume, 50 mM Tris pH 8.0, 600 mM NaCl, 1% IGE-PAL, 0.1% BSA, 1 mM DTT, 1.0 mM EDTA, 250 mM NaF, 0.1 mM sodium vandate, 5 µg/ml pepstatin A, 12 µg/ml leupeptin, 1.5 mM AEBSF, 7 µg/ml aprotinin, 65 µM bestatin, and 7 µM E-64). The cell lysate was then centrifuged at 20,000 x g for 30 minutes at 4° C, and the resulting pellet discarded. The remaining cell lysate supernatant fraction was

subjected to a pre-clearing step to reduce non-specific protein interactions by incubating the cell lysate with pre-immune antibody resin for 30 minutes at 4°C. [Prior to use, the antibody resin was washed with an antibody wash buffer (50 mM Tris pH 8.0, 150 M NaCl, 0.1% IGE-PAL, 1mM DTT, 0.2% BSA)]. After the pre-clearing incubation step, the mixture was centrifuged at 6000 x g for 5 minutes at 4°C, and the resin was discarded.

The pre-cleared lysate was then added (1:1 ratio, volume/volume) to an IGE-PAL assay buffer containing proteinase and phosphatase inhibitors (50 mM Tris pH 8.0, 1% IGE-PAL, 0.1% BSA, 1 mM DTT, 2.5 mM EDTA, 250 mM NaF, 0.1 mM sodium vandate, 9 μg/ml pepstatin A, 10 μg/ml leupeptin, 4.5 mM AEBSF, 9 μg/ml aprotinin, 260 μM bestatin, and 28 μM E-64). Fifty microliteres of antibody resin, that had previously been washed with antibody wash buffer, was then added to the mixture and incubated for 2 hours at 4°C. Control samples were incubated with pre-immune antibody resin instead of immune resin. After the incubation step, the mixture was centrifuged at 6000 X g for 1 minute at 4°C and the supernatant discarded. The resin was washed three times with radioimmunprecipitation assay buffer (RIPA) (50 mM Tris pH 8.0, 150 mM NaCl, 1% IGE-PAL, 0.5% deoxycholate, 0.1% SDS) and a centrifugation step (6000 x g for 1 min at room temperature). The resin was then transferred to a mini-column and washed with a 10ml of RIPA wash buffer. Proteins bound by the antibody resin were eluted from the matrix by adding 40 μl elution buffer (62.5 mM Tris pH 6.8, 4% SDS) and incubating at 100°C for 1 minute. The mini-columns were centrifuged at 6000 x g for 2 minutes at room temperature to collect the eluted material. The eluted proteins were then lyophilized using a centrifugal Speed-Vac Concentrator (Savant, Farmingdale, NY) and resolubalized in 1X SDS sample buffer (62.5 mM Tris pH 6.8, 2% SDS, 10% glycerol, 0.5% BME, and bromphenol blue) and stored at -20°C for later use in Western Immunoblot and silver stained SDS-PAGE analysis.

Western Immunoblot

For Western Immunoblot analysis, the co-immunoprecipitated protein products were electrophoretically separated using a 12.5% sodium dodecyl sulfate polyacrylamide gel (SDS-PAGE 8x10x0.15 cm gel) and a SE600 Gel Electrophoresis Apparatus (Hoefer SE600). The proteins were then transferred from the gel onto a polyvinylidene difluoride (PVDF) membrane using an electroblotting unit (Hoefer TE22 Transfer Unit, Holliston, MA). The protein transfer step was performed at 50 volts for 3 hours at 20°C using Towbin's Transfer Buffer (25 mM Tris, 192 mM glycine, 20% methanol, and 0.1% SDS, pH 8.2) (55). Afterwards, the membrane was incubated overnight at room temperature in a blocking solution containing 3% gelatin solubalized in Tween-Tris Buffered Saline (TTBS) (20mM Tris pH 7.5, 500mM NaCl, 0.05% Tween 20). After the blocking step, the membrane was washed with TTBS followed by incubation with the primary antibody [rabbit anti-cTHY28 (1:500) or chicken anti-GFP (1 μg/ml)] diluted in primary antibody buffer (TTBS, 1% goat or rabbit serum) for 2 hours at room temperature. After this incubation step, the membrane was washed three times with TTBS and then incubated with secondary antibody (goat, anti-rabbit IgG alkaline phosphatase conjugate or rabbit, anti-chicken IgY alkaline phosphatase conjugate) diluted to 1:5000 in secondary antibody buffer (dH_20, 1% BSA, 20 mM Tris pH 8.5, 145 mM NaCl, 0.05% Tween 20, 1% goat or rabbit serum) for two hours at room temperature. The membrane was then washed three times with TTBS, and the immunoreactive protein bands were visualized by adding a chromogenic substrate solution (100 mM Tris pH 9.5, 100mM NaCl, 5mM $MgCl_2$, 330 μg/ml nitro-blue tetrazolium chloride, and 170 μg/ml 5-bromo-4-chloro-3'-indolyphosphate-p-toluidine salt).

Densitometric Scanning

Densitometric scanning of Western Immunoblots was performed, as previously described in (1), using a Bio-Rad Gel Doc Imaging System and Molecular Analyst Software (Hercules, CA) according to the manufacturer's recommendations.

Protein Visualization by Silver Staining

A SDS-PAG silver staining procedure was used to analyze the co-immunoprecipitated protein products. Proteins that were eluted from the antibody resin were electrophoretically separated on a 12.5% sodium dodecyl sulfate polyacrylamide gel (SDS-PAG 8x10x0.15 cm gel). The gel was then fixed in a 50% methanol, 5% acetic acid solution for 15 minutes at room temperature. The gel was subsequently washed in 50% methanol for 10 minutes at room temperature. The gel was then allowed to incubate in H_2O overnight at room temperature to reduce background staining. The gel was sensitized in a 0.02% solution of $Na_2S_2O_3$ for one minute, followed by two H_2O washes for one minute each at room temperature. The gel was then stained with 0.1% $AgNO_3$ for 20 minutes at 4° C, followed by two more washes in H_2O for one minute each at room temperature. The proteins were then visualized by adding a 0.04% formalin, 2% Na_2CO_3 solution. For mass spectrometric analysis, the protein bands of interest were excised from the gel and stored at -20°C in acetonitrile-washed micro-centrifuge tubes.

Protein Sample Preparation for Mass Spectrometric Analysis

To prepare protein samples for mass spectrometric analysis, an in-gel tryptic digest protocol was used (56). The protein bands of interest from a single silver-stained gel were destained using a 1:1 mixture (volume/volume) of 30 mM potassium ferricyanide and 100 mM sodium thiosulfate. The gel bands were subsequently washed three times with water at room temperature and diced into 1 mm cubes. The diced gel slices were dehydrated by incubating

with a solution of 50% acetonitrile and 50 mM NH_4HCO_3 (pH 8.0) for 15 minutes at room temperature. This solution was removed and replaced with 100% acetonitrile and incubated for 5 minutes at room temperature. The diced gel slices were then dried in a centrifugal Speed-Vac Concentrator.

The proteins in the diced gel slices were then subjected to a reduction step by adding a solution of 10 mM DTT and 50 mM NH_4HCO_3 (pH 8.0) and incubating at 56°C for 45 minutes. To alkylate the proteins in the gel slices, the reduction solution was removed and replaced with a solution of 55mM iodoacetamide in 50 mM NH_4HCO_3 (pH 8.0) and incubated for 60 minutes at room temperature. The alkylation solution was removed and the gel slices were washed with 50 mM NH_4HCO_3 (pH 8.0) for 5 minutes at room temperature. The diced gel slices were then subjected to a dehydration step as described previously.

The in-gel tryptic digest of the proteins was performed by adding 20 μg/ml trypsin in 10% acetonitrile and 40 mM NH_4HCO_3 (pH 8.0) and incubating at 4° C for 45 minutes. At the end of the incubation period, the trypsin solution was removed and the gel slices were incubated with an elution buffer (50mM NH_4HCO_3, pH 8.0) overnight at 37°C. This elution fraction was collected and saved for mass spectrometric analysis. To extract tryptic peptides from the diced gel slices, H_2O was added to the sample tube and placed in a sonication bath for 10 minutes at room temperature. This elution fraction was removed and saved for mass spectrometric analysis. To further extract tryptic peptides from the diced gel slices, a third elution solution (50% acetonitrile and 5% formic acid) was added to the sample tube and placed in a sonication bath for 10 minutes at room temperature. This extraction step was repeated, and the extracted tryptic peptides in the elution fractions were pooled together, and lyophilized using a centrifugal Speed-Vac concentrator.

The tryptic peptides were subjected to a final purification step using Zip-Tips (C18 reverse phase chromatography matrix) according to manufacturer's recommendations (Millipore Corporation, Billerica, MA). The Zip-Tip was equilibrated with a solution of 0.1% trifluoroacetate and 1M guanidine HCl. The tryptic peptide samples were solubalized in this equilibration solution and bound to the Zip-Tip matrix. The Zip-Tip matrix was then washed with a 5.0% methanol and 0.1% TFA solution. The tryptic peptides were eluted from the Zip-Tip matrix using a 50% acetonitrile and 0.1% TFA solution. A second elution step, using a solution of 75% acetonitrile and 0.1% TFA, was performed. The eluted tryptic peptides were pooled and lyophilized using a centrifugal Speed-Vac Concentrator.

Mass Spectrometric Analysis

The peptides from each sample were analyzed in duplicate. An Agilent 1100 capillary liquid chromatography system (Palo Alto, CA) was attached to the mass spectrometer (Thermo Fisher, San Jose, CA) *via* a T splitter to allow infusion at micro liter flow rates (57). A five-micrometer-diameter C18 matrix (Rainin, Woburn, MA) was packed into a pulled fused-silica capillary (10.5 cm×100 μm id) under 1000 psi pressure using nitrogen gas. Peptide samples were loaded onto the column for 45 minutes under the same pressure. Peptides were then eluted with a gradient using 0.1% formic acid (buffer A) and 99.9% acetonitrile/0.1% formic acid (buffer B). Following the initial wash with 95% buffer A for 10 minutes, peptides were eluted from the column with a 90 minute linear gradient of 5–60% of buffer B at a flow rate of ~200 μl /min directly into an LTQ linear ion trap mass spectrometer (Thermo Fisher, San Jose, CA) using a voltage of 2500 V.

The instrument was set to acquire MS/MS spectra on the nine most abundant precursor ions from each MS scan with a repeat count set of 3 and repeat duration of 5 seconds. Dynamic

exclusion was enabled for 160 seconds. Raw tandem mass spectra were converted into a peak list using Read followed by mzMXL2Other algorithms (58). The peak lists were then searched using Mascot 1.9 software program (Matrix Science, Boston, MA).

For database searching and protein identification, a target database was created containing all proteins predicted for the *Gallus gallus* genome. In addition, a decoy database was then constructed by reversing the sequences in the normal database. Searches were performed against the target and decoy databases using the following parameters: (i) fully tryptic enzymatic cleavage with two possible missed cleavages, (ii) peptide tolerance of 800 parts-*per*-million, (iii) fragment ion tolerance of 0.8 Da, and (iv) variable modifications due to carboxyamidomethylation of cysteine residues (+57 Da) and deamidation of asparagine residues (+1 Da). Following the database searches, statistically significant proteins were determined for each sample at a 1% protein false discovery rate using the Provalt algorithm as implemented in ProteoIQ (BioInquire, LLC, Athens) (59). Provalt parsimoniously clusters non-redundant peptides falling within the user-defined criteria to protein homology groups based on sequence homology of identified peptides. The protein with the most sequence coverage is reported as the top scoring protein.

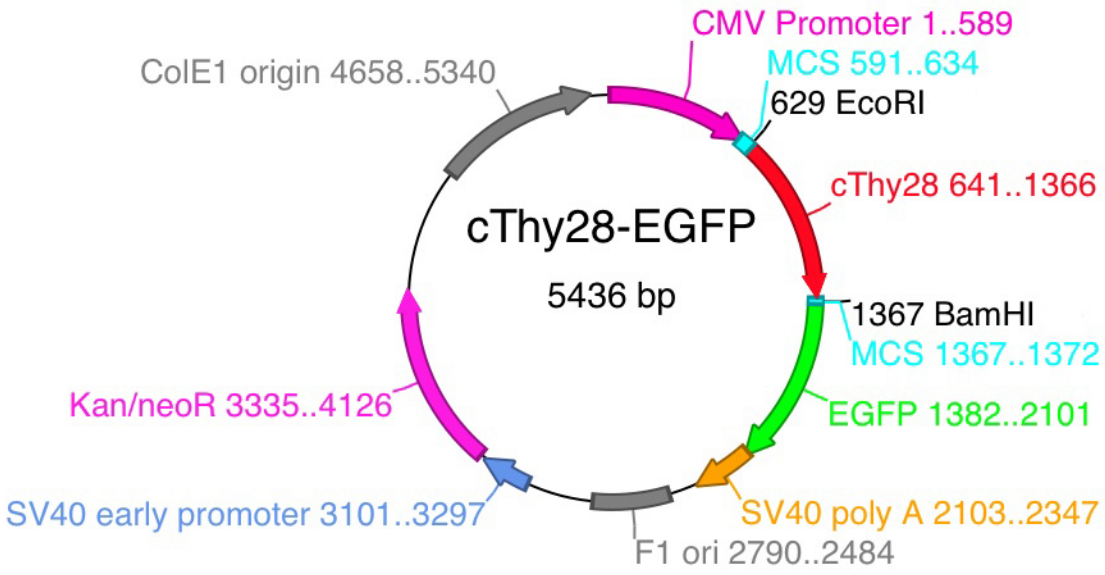

Figure 1: Generation of cThy28/EGFP Fusion Construct. The coding sequence for the cThy28 gene was inserted into the EcoR1/BamH1 multicloning site of the pEGFP-N3 N-Terminal Protein Fusion Vector. ColE1 origin-*E.coli* origin of replication; CMV Promoter-Human cytomegalovirus immediate early promoter; MCS- multicloning site; EGFP- Enhanced Green Fluorescent Protein; SV40 poly A-Simian Virus 40 early mRNA polyadenylation signal; F1 ori-F1 Filamentous phage single-strand DNA origin; SV40 early promoter-Simian Virus 40 early promoter; Kan/neoR- Kanamycin/neomycin resistance gene.

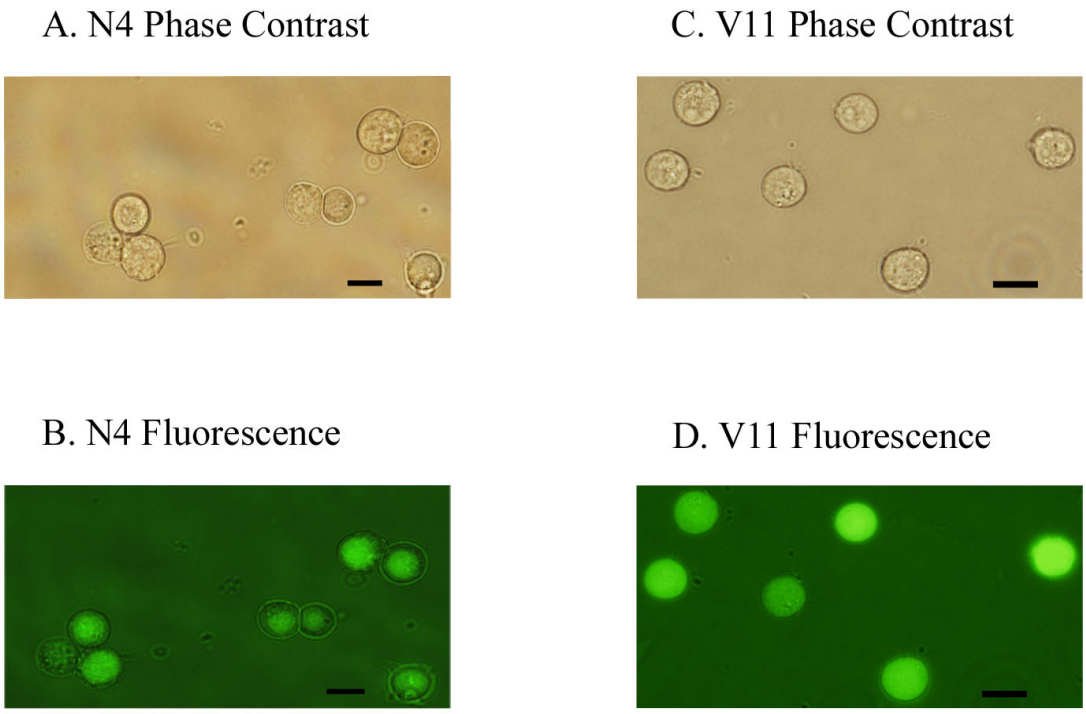

Figure 2: EGFP expression in DT-40 cell lines. Panels A (Phase Contrast) and B (Fluorescence) demonstrate the expression and nuclear localization of the cTHY28/EGFP fusion protein in the DT-40 N4 cell line. Panels C (phase contrast) and D (Fluorescence) demonstrate cellular expression of the EGFP protein in the DT-40 V11 cell line. The black scale bar located in the right hand corner of each panel represents 10μm.

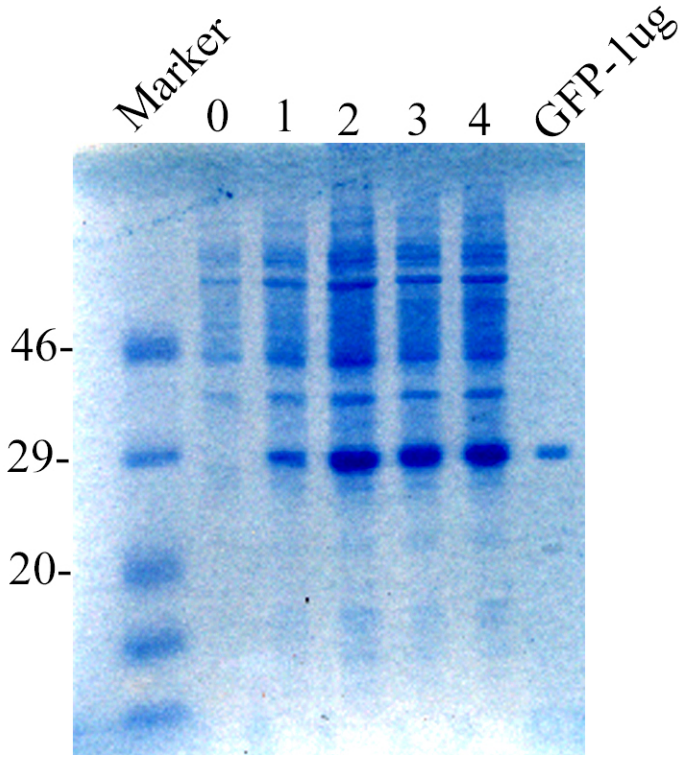

Figure 3: Time Course of bacterial expression of GFP and purification using metal chelation affinity chromatography. Aliquots of the bacterial culture were collected at 0, 1, 2, 3, and 4 hours after induction with 1mM IPTG (isopropyl β-D-thiogalactopyranoside) and analyzed by SDS-PAGE and Coomassie Blue staining. 1μg of the affinity purified GFP protein is shown in the outer lane on the right and molecular weight markers expressed in kilodaltons are indicated on the left.

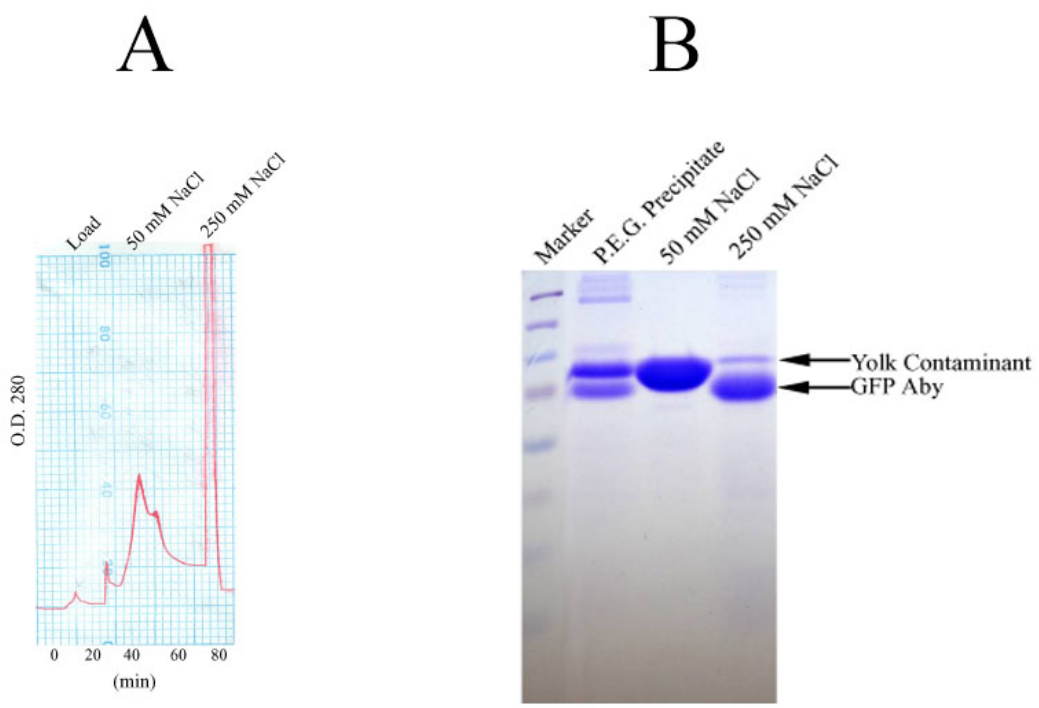

Figure 4: Purification Chicken anti-GFP antibodies. Panel A represents a chromatogram of antibody purification using DEAE column chromatography. The vertical axis represents relative protein concentration as determined by O.D. 280, and the horizontal axis represents elution time in minutes. The Load peak represents the P.E.G. precipitated yolk proteins that were applied to the DEAE column, but did not bind to the matrix. The 50 mM NaCl fraction represents non-IgY yolk proteins that were eluted from the column using 50 mM NaCl. The 250 mM NaCl fraction represents material that was eluted from the column using 250 mM NaCl which is enriched in IgY proteins. Panel B represents an analysis of the DEAE column fractions using SDS-PAGE and Coomassie Blue staining. Molecular weight markers expressed in kilodaltons are indicated on the left. The P.E.G. Precipitate lane represents yolk proteins that were precipitated using 9% P.E.G. The 50 mM NaCl lane represents non-IgY yolk proteins that were eluted from the column using 50 mM NaCl. The 250 mM NaCl lane represents material that was eluted from the column using 250 mM NaCl which is enriched in IgY. The Yolk Contaminant represents a non-IgY yolk protein present in the P.E.G. Precipitate. The GFP Aby (Antibody) represents the IgY antibody heavy chain found in the 250 mM NaCl Fraction. Approximately 10 µg of protein (except of marker lane) was loaded per lane. The molecular weight of the marker proteins are 260 kDa, 140 kDa, 100 kDa, 70, kDa, 50 kDa, 40 kDa, 35 kDa, 25 kDa.

CHAPTER 3: RESULTS

Optimization of Formalin Cross-Linking Conditions for Co-Immunoprecipitation Assay

To optimize conditions for the co-immunoprecipitation assay, various concentrations (0, 0.065, 0.125, 0.250, 0.375, and 0.500%, with an incubation time of 10 minutes) of formalin, were employed to enhance the cross-linking of interacting proteins with cTHY28 (Figures 5 and 6). Pre-immune anti-GFP antibody resin was used to detect non-specific binding proteins, in cells that had been treated with 0% and 0.5% levels of formalin. Relatively low levels of non-specific protein binding (56 kDa and 22 kDa protein bands) were observed in both the pre-immune and immune lanes. Presumably, the non-specific 56 kDa protein band was masked by the intense staining of the fusion protein band in the immune lanes. As expected, the most prominent protein detected using this anti-GFP immune antibody resin was the ~57kDa cTHY28/EGFP fusion protein. Interestingly, immunoprecipitation of the fusion protein was optimized when 0%, 0.375%, and 0.5% concentrations of formalin cross-linking reagent were employed. It was also observed that the relative concentration of an ~38 kDa protein band (a putative degradation product of the ~57kDa fusion protein) that was detected in the immune samples appears to parallel the relative concentration of the ~57 kDa fusion protein band. The prominent ~120 kDa band along with a cluster of five protein bands ranging in molecular weight of ~135-200 kDa (putative cTHY28 interacting proteins that have been cross-linked to the cTHY28/EGFP fusion protein) demonstrate a clear increase in relative abundance as a function of the formalin concentration (densitometric scanning data, Figure 6). In addition, a ~260 kDa protein band (putative cTHY28 interacting proteins that have been cross-linked to the

cTHY28/EGFP fusion protein) was detected at the 0.250% level of formalin concentration. There was an increase in the relative abundance of this protein band at the 0.375% and 0.5% concentrations of formalin (densitometric scanning data, Figure 6). The pattern of high molecular weight protein bands (~120-200 kDa) observed in the 0% formalin concentration immune sample was unlike that observed in the other samples. This observation suggests that the formalin cross-linking procedure enhanced the formation of protein complexes that interact with the fusion protein. Furthermore, several lower molecular weight protein bands (~52 kDa and 44 kDa) were observed in the 0% formalin immune sample. Presumably, these proteins represent degradation products of the ~57 kDa fusion protein. The 0.25% concentration was chosen as the optimum formalin concentration for further experiments due to the number of clarity of the bands displayed on the Western Immunoblot.

In addition to optimizing formalin concentrations for the co-immunoprecipitation assay, a time course of formalin cross-linking (0, 5, 10, 15, 20, 30 minutes, with 0.25% formalin) was performed to enhance the cross-linking of interacting proteins with cTHY28 (Figures 7 and 8). Similar to Figure 5, relatively low levels of non-specific protein binding (56 kDa and 22 kDa protein bands) were observed in both the pre-immune and immune lanes. Presumably, the non-specific ~56 kDa protein band was masked by the intense staining of the fusion protein band observed in the samples receiving the anti-GFP immune antibody resin. As observed in Figure 5, the most prominent protein band detected using this anti-GFP immune antibody resin in Figure 7 was the ~57kDa cTHY28/EGFP fusion protein. Interestingly, the highest levels of this protein were observed at the 0 minute time point. As shown in the densitometric scanning data (Figure 8), there was a slight decline in the relative quantities of the fusion protein as a function of formalin cross-linking time. Likewise, the relative concentration of the putative degradation

products of the ~57kDa fusion protein (~52 and ~38 kDa protein bands) appears to parallel the modest decline of the ~57 kDa fusion protein band as a function of time. The relative concentration of the putative cTHY28 interacting proteins (120, 135-200, and 260 kDa protein bands) increased from 0 minutes to 15 minutes; however, from 15 minutes to 30 minutes, a slight decline in the concentration of these protein bands was observed (Figure 8). The pattern of high molecular weight protein bands (120-260 kDa) found in the 0 minute immune sample is unlike that observed in the 5-30 minute formalin cross-linked samples, suggesting that the formalin cross-linking procedure appears to enhance the formation of protein complexes that interact with the fusion protein.

Analysis of Co-Immunoprecipitated Products in DT-40 Cell Lines

To confirm the specificity of the putative cTHY28 interacting protein bands observed during the optimization of formalin cross-linking, the DT-40 N4, WT, and V11 cell lines, and two different antibodies (chicken, anti-GFP and rabbit, anti-cTHY28) were employed (Figure 9, Panels A and B). In Panel A of Figure 9, the immunoprecipitation assay and the Western Immunoblot analysis were preformed using chicken, anti-GFP antibodies whereas, rabbit, anti-cTHY28 antibodies were used in Panel B. The pattern of protein bands generated by the chicken, anti-GFP pre-immune antibody resin was similar among all three cell lines (Panel A). The 72 kDa and ~20-30 kDa protein bands, detected in the pre-immune antibody resin may represent chicken IgY heavy and light chains, respectively. These antibody proteins may have been stripped from the antibody resin during the elution step of the co-immunoprecipitation procedure and detected by the secondary antibody in the Western Immunoblot analysis. When DT-40 N4 cells that expressed the cTHY28/EGFP fusion protein were analyzed, the 57 kDa fusion protein was readily detected, along with the putative cTHY28 interacting proteins as

previously observed in Figures 5 and 7. This pattern of cTHY28 interacting protein bands was not observed in DT-40 WT cells or DT-40 V11 cells that express the EGFP protein alone. In fact, the pattern of protein bands observed for the DT-40 WT cells treated with the pre-immune or immune anti-GFP resin was virtually identical. On the other hand, the EGFP protein band (27 kDa) was readily detected, as expected, when the immune anti-GFP resin was employed. Likewise, a 54 kDa protein band was observed in this sample that most likely represents a EGFP dimer. The putative cTHY28 interacting proteins (120-260 kDa) were not detected in the DT-40 V11 cell lysates.

In Panel B, the pattern of protein bands generated by the rabbit, anti-cTHY28 pre-immune antibody resin was similar for the DT-40 WT and V11 cell lines. The 56 kDa and 20-25 kDa protein bands detected by the pre-immune resin may represent rabbit heavy and light chain antibody proteins, respectively. As observed in Panel A, these antibody proteins may have been stripped from the antibody resin during the elution step of the co-immunoprecipitation procedure and detected by the secondary antibody used in the Western Immunoblot analysis. Unlike the DT-40 WT and V11 cells a non-specific 57 kDa protein band was observed in DT-40 N4 cells when the rabbit, anti-cTHY28 pre-immune resin was employed. The source of this protein band is unknown. When DT-40 N4 cells that expressed the cTHY28/EGFP fusion protein were analyzed, the 57 kDa fusion protein was readily detected, along with the putative cTHY28 interacting proteins, and the endogenous cTHY28 protein band. An additional ~40kDa protein band was detected in this sample. This protein band may represent a degradation product of the fusion protein. When cell lysates were prepared from the DT-40 WT and V11 cell lines, the endogenous cTHY28 was readily detected using the co-immunoprecipitation assay; however, significant amounts of putative cTHY28 interacting proteins were not observed when the rabbit

anti-cTHY28 immune resin was employed. Based on this observation, it would appear that the over-expression of the cTHY28/EGFP fusion protein may favor the formation and detection of putative cTHY28 interacting proteins.

Isolation of Putative cTHY28 Interacting Proteins for Mass Spectrometric Analysis

To generate sufficient quantities of the cTHY28/EGFP fusion and putative cTHY28 interacting proteins, a cell lysate was prepared from ~10 liters of DT-40 N4 cells. The formalin cross-linked immunoprecipitated proteins were recovered from the lysate using the chicken, anti-GFP antibody resin and electrophoretically separated on an SDS-PAG gel. The immunoprecipitation protocol was performed using both pre-immune and immune antibody resins. Protein bands were visualized using a silver stain procedure, and putative cTHY28 interacting protein bands generated from the immune antibody resin were excised from the gel (Figure 10). As a control, comparable areas of the gel were excised from the gel lanes that contained cell lysates that had been subjected to immunoprecipitation using the chicken, anti-GFP pre-immune antibody resin. Relatively large amounts of the cTHY28/EGFP fusion protein were readily detected in the silver-stained gel and excised from the gel matrix. Reduced amounts of putative cTHY28 interacting bands (95, 120, and 200 kDa) were detected and excised from the gel. Unexpectedly, the pattern of silver-stained, putative cTHY28 interacting bands was not identical to the pattern found in the Western Immunoblot (Figure 9). This discrepancy most likely reflects a difference in the relative detection limits of the silver-stain technique and the Western Immunoblot procedure.

Identification of Putative cTHY28 Interacting Proteins

Mass spectrometric analysis of protein complexes represents a powerful means of detecting and identifying small amounts of protein that are present in immunoprecipitated

material (60). In this study, high pressure, reverse phase capillary liquid chromatography in conjunction with a LTQ mass spectrophotometer was used to identify immunoprecipitated proteins that were visualized in silver-stained SDS-PAGE gel bands. Using this methodology, the antibody target protein, cTHY28, was exclusively detected in samples generated by the immune antibody resin, thereby confirming the validity of this assay procedure (Table 1). In addition to cTHY28, this analysis revealed the presence of 42 other proteins that were present in the immune co-immunoprecipitated samples. The vast majority of these proteins represent non-specific protein interactions with the antibody resin since they were detected in the samples generated using both the pre-immune and immune antibody resin. However, there were three proteins (Nucleolin, DNA Topoisomerase 1, and Elongation Factor-2) that were detected exclusively in the samples generated using the immune antibody resin as shown in Table 1.

Based on the number of nucleolin tryptic peptides (15), percent sequence coverage (20.3), and MASCOT score (745.4), this protein was the most prevalent cTHY28 interacting protein detected in the immunoprecipitated complex. The second most prevalent interacting protein detected was DNA topoisomerase 1 (12 tryptic peptides, 15.0 percent sequence coverage and 515.4 MASCOT score), followed by elongation factor-2 (9 tryptic peptides, 12.3 percent sequence coverage and 437.0 MASCOT score).

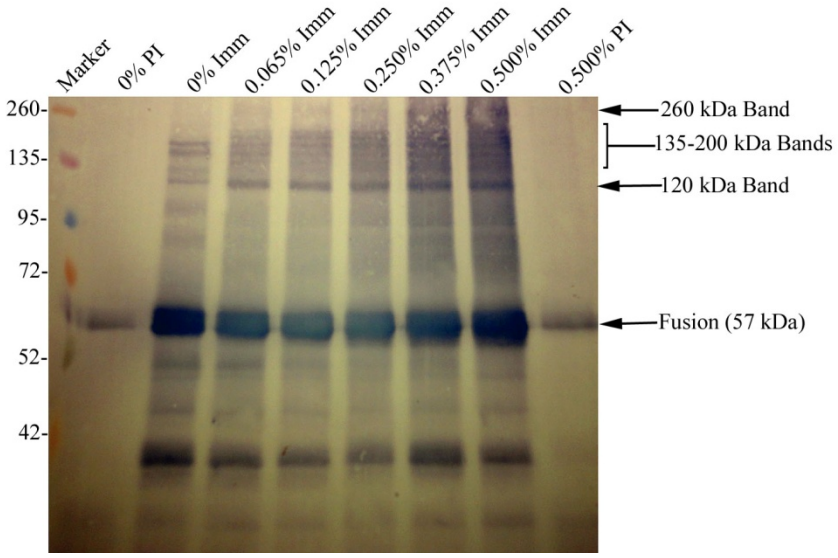

Figure 5: Western Immunoblot analysis of dose-dependent formalin cross-linking of immunoprecipitated proteins from DT-40 N4 cells. DT-40 N4 cells were treated with increasing amounts of formalin (0%, 0.065%, 0.125%, 0.250%, 0.375%, and 0.500%) for 10 minutes and a cell lysate was prepared. A co-immunoprecipitation procedure using the GFP antibody matrix (PI- Pre-Immune GFP antibody matrix; Imm- Immune GFP antibody matrix) was performed on these cellular lysates, and subjected to Western Immunoblot analysis using the rabbit α-cTHY28 antibody. Fusion (57 kDa)- cTHY28/EGFP fusion protein; 120 kDa Band, 135-200 kDa Bands, 260 kDa Band- potential cTHY28 interacting proteins. Molecular weight markers expressed in kilodaltons are indicated on the left.

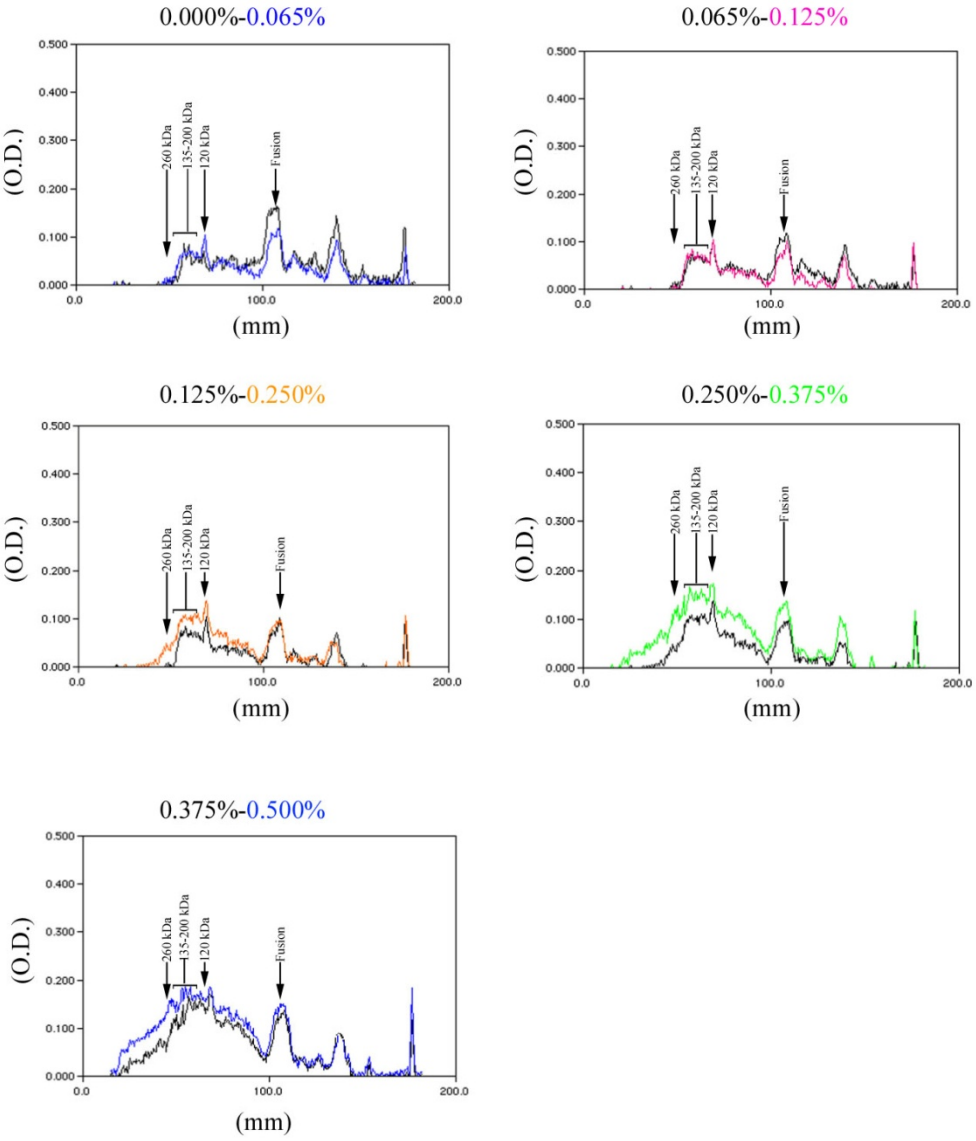

Figure 6: Densitometric scan of the Western Immunoblot analysis shown in Figure 5. Panels A (0%-0.065%), B (0.065%-0.125%), C (0.125%-0.250%), D (0.250%-0.375%), and E (0.375%-0.500%) represent densitometric scans that compare formalin cross-linked immunoprecipitated proteins in adjacent lanes of Figure 5. The vertical axis represents relative O.D. and the horizontal axis represents blot length (mm). Fusion- cTHY28/EGFP fusion protein; 120 kDa, 135-200 kDa, 260 kDa- potential cTHY28 interacting proteins.

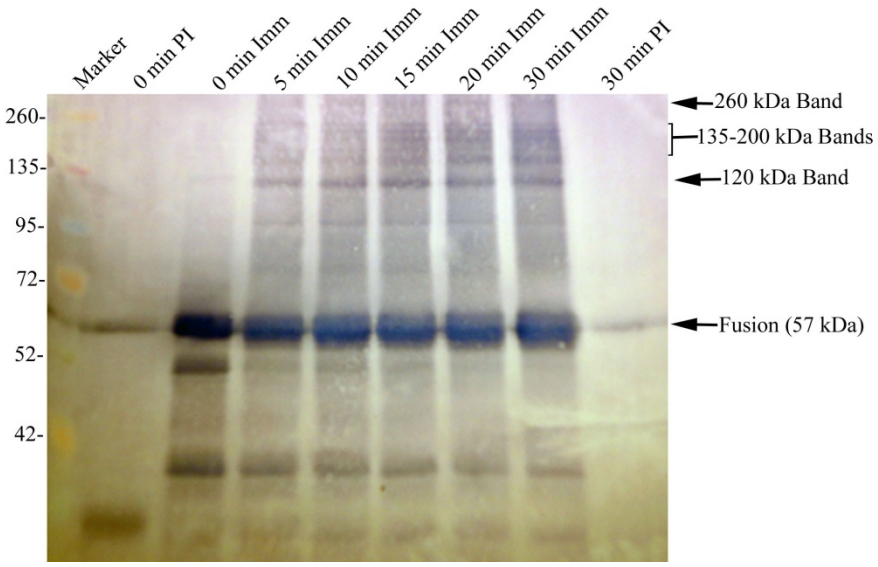

Figure 7: Western Immunoblot analysis of time-dependent formalin cross-linking of immunoprecipitated proteins from DT-40 N4 cells. DT-40 N4 cells were treated with 0.250% formalin for increasing amounts of time (0 minutes, 5 minutes, 10 minutes, 15 minutes, 20 minutes, and 30 minutes) and a cell lysate was prepared. A co-immunoprecipitation procedure using the GFP antibody matrix (PI- Pre-Immune GFP antibody matrix; Imm- Immune GFP antibody matrix) was performed on these cellular lysates, and subjected to Western Immunoblot analysis using the N3 antibody. Fusion (57 kDa)- cTHY28/EGFP fusion protein; 120 kDa Band, 135-200 kDa Bands, 260 kDa Band- potential cTHY28 interacting proteins. Molecular weight markers expressed in kilodaltons are indicated on the left.

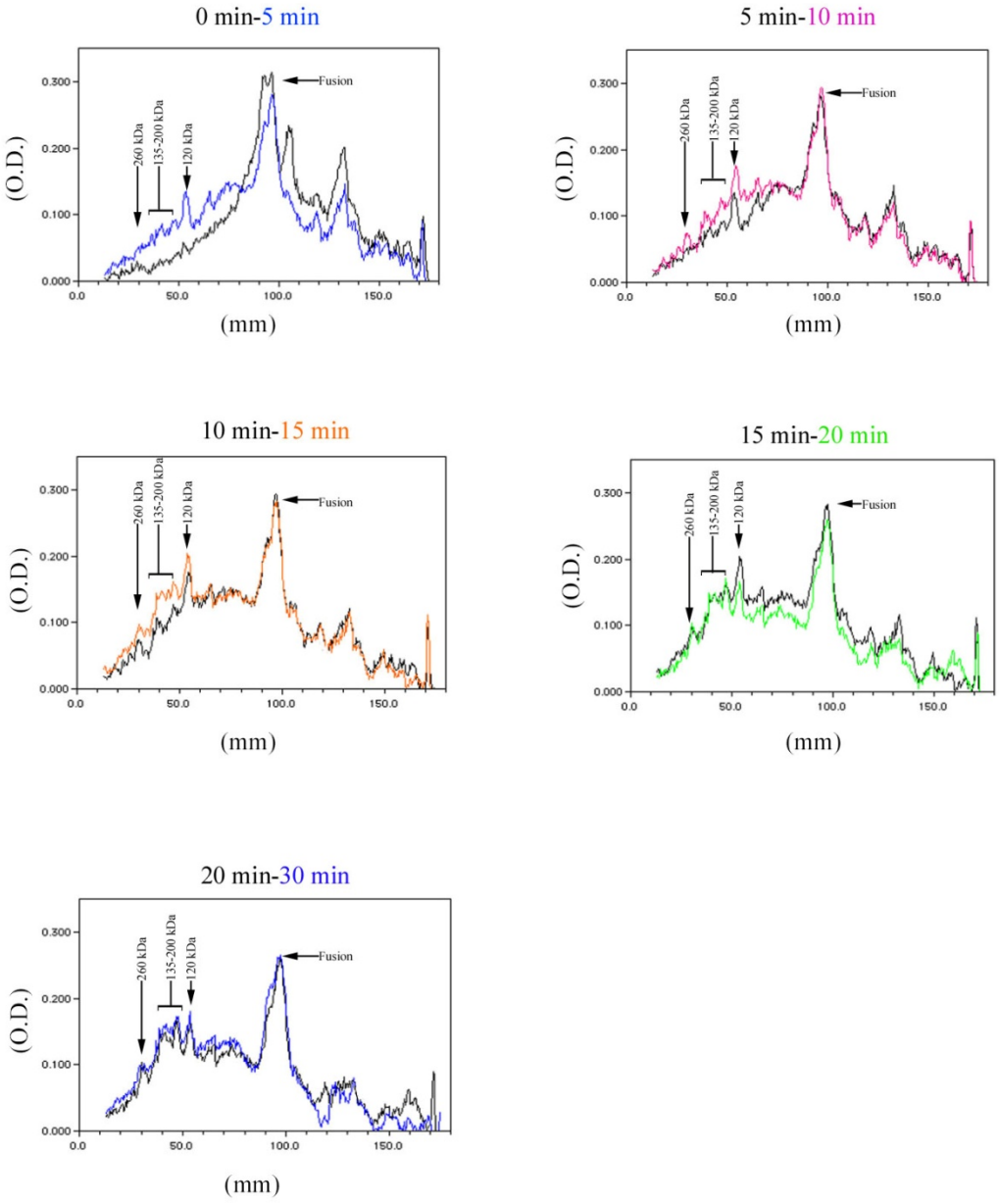

Figure 8: Densitometric scan of the Western Immunoblot analysis shown in Figure 7. Panels A (0 min-5 min), B (5 min-10 min), C (10 min-15 min), D (15 min-20 min), and E (20 min-30 min) represent densitometric scans that compare formalin cross-linked immunoprecipitated proteins in adjacent lanes of Figure 7. The vertical axis represents relative O.D. and the horizontal axis represents blot length (mm). Fusion- cTHY28/EGFP fusion protein; 120 kDa, 135-200 kDa, 260 kDa- potential cTHY28 interacting proteins.

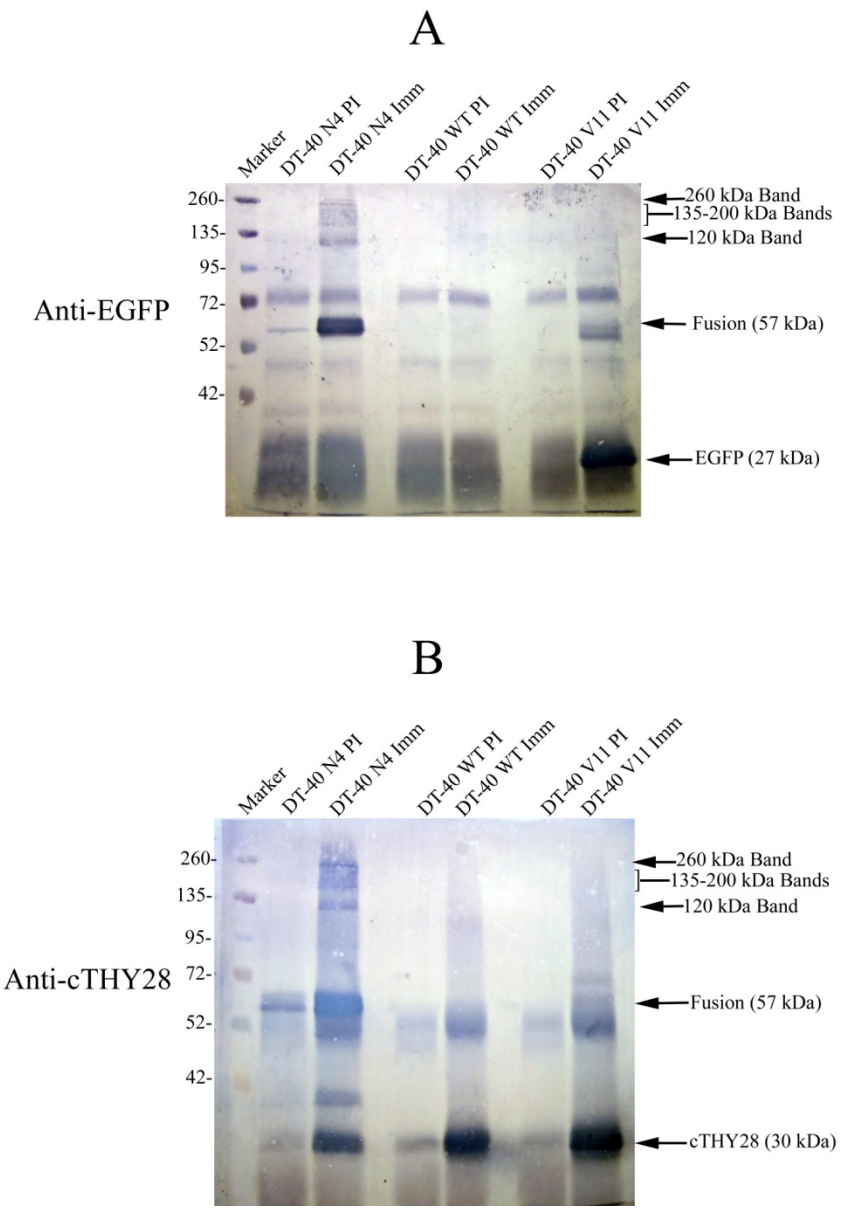

Figure 9: Western Immunoblot analysis of formalin cross-linked, immunoprecipitated proteins from DT-40 cell lines. DT-40 cell lines (N4, WT, V11) were treated with 0.250% formalin for 10 minutes and a cell lysate was prepared. A co-immunoprecipitation procedure using the GFP antibody matrix (PI- Pre-Immune GFP antibody matrix; Imm- Immune GFP antibody matrix) was performed on these cellular lysates, and subjected to Western Immunoblot analysis using the GFP antibody (Panel A). A co-immunoprecipitation procedure using the N3 antibody matrix (PI- Pre-Immune N3 antibody matrix; Imm- Immune N3 antibody matrix) was performed on these cellular lysates, and subjected to Western Immunoblot analysis using the N3 antibody (Panel B). Fusion (57 kDa)- cTHY28/EGFP fusion protein; 120 kDa Band, 135-200 kDa Bands, 260 kDa Band- potential cTHY28 interacting proteins; EGFP (27 kDa)- EGFP; cTHY28 (30 kDa)- cTHY28. Molecular weight markers expressed in kilodaltons are indicated on the left.

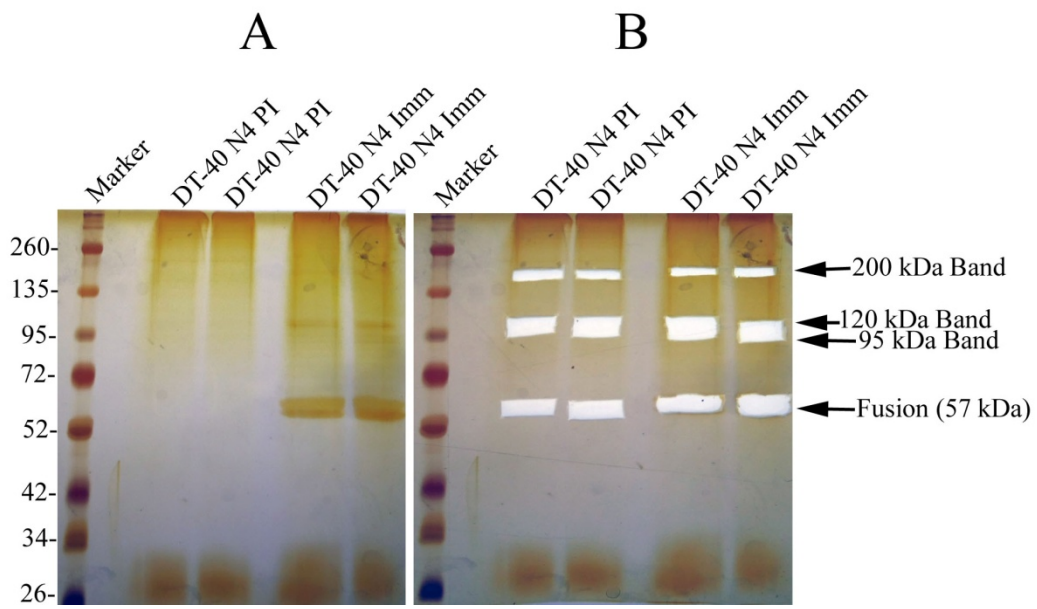

Figure 10: Silver Stain analysis of formalin cross-linked, immunoprecipitated proteins from DT-40 N4 cells. DT-40 N4 cells were treated with 0.250% formalin for 10 minutes and a cell lysate was generated. A co-immunoprecipitation procedure using the GFP antibody matrix (PI- Pre-Immune GFP antibody matrix; Imm- Immune GFP antibody matrix) was performed on these cellular lysates, and subjected to SDS-PAGE and silver staining (Panel A). Bands of interest were excised from the gel for use in subsequent mass spectrometric analysis (Panel B). Fusion (57 kDa)- cTHY28/EGFP fusion protein; 95 kDa Band, 120 kDa Band, 200 kDa Band- potential cTHY28 interacting proteins. Molecular weight markers expressed in kilodaltons are indicated on the left.

Table 1. Mass Spectrometric Analysis of the cTHY28 Co-Immunoprecipitated Material.

Gel Band	Peptide Sequence	Protein Group	% Sequence Coverage	MASCOT Score
5 (Immune 200 kDa)	AQPNQTTFWEGVR	cTHY28	5.37	41.75
6 (Immune 120 kDa)	AQPNQTTFWEGVR	cTHY28	8.26	70.6
	FSIEDLK			
	AMVIDYTGEK	Nucelolin	20.32	718.15
	EALNSCNNTEIEGR			
	FGYVDFLSAEDMDK			
	GFGFVDFSSPEDAK			
	GLSEDTTEETLR			
	GYAFVEFPTAEDAK			
	KTETPASAFSLFVK			
	LEFSSPSWQK			
	NLQVSEVR			
	NLTPTKDYEELR			
	NVFENALEVR			
	TETPASAFSLFVK			
	VTLDFAKPK			
	AEEVATFFAK	DNA Topoisomerase 1	15.01	493.18
	ELTNPDDNIPAK			
	GPVFAPPYEPLPENVK			
	LEVQATDREENK			
	LNTSILNK			
	MLDHEYTTK			
	NLQLFMENK			
	QIALSTSK			
	QPEDDLFDR			
	TYNASITLQQQLK			
	YIMLNPSSR			
	AYLPVNESFGFTADLR	Elongation Factor-2	10.26	386.11
	EDLYLKPIQR			
	ETVSEESNVMCLSK			
	GHVFEESQVAGTPMFVVK			
	IMGPNYTPGK			
	VFSGLVSTGLK			
	VNFTVDQIR			
7 (Immune 95 kDa)	AQPNQTTFWEGVR	cTHY28	5.37	38.08
	GFGFVDFSSPEDAK	Nucelolin	3.89	113.07
	TETPASAFSLFVK			
	GPVFAPPYEPLPENVK	DNA Topoisomerase 1	3.79	111.01
	TYNASITLQQQLK			
	AYLPVNESFGFTADLR	Elongation Factor-2	1.86	72.54
8 (Immune 57 kDa)	AQPNQTTFWEGVR	cTHY28	36.78	803.82
	EAYPDHTQFDQK			
	EAYPDHTQFDQKDPHYDSSSR			
	EPGIVGIVK			
	FIPLSEIK			
	FSIEDLK			
	FSIEDLKAQPNQTTFWEGVR			
	LGQQAFFYHSNCK			
	LGQQAFFYHSNCKEPGIVGIVK			
	NMMLFSR			
	RFIPLSEIK			
	WSMVDVQFVR			

CHAPTER 4: DISCUSSION

The experiments described in this thesis were designed to identify cellular proteins that specifically interact with cTHY28. To optimize the detection of these interacting proteins, the following strategies were employed:

1. Employ a source of cells that express high levels of cTHY28 (DT-40 N4 cell line).
2. Employ a sensitive methodology that is capable of detecting low levels of cTHY28 interacting proteins (Co-Immunoprecipitation).
3. Employ a procedure where assay conditions can be optimized to detect proteins that specifically interact with cTHY28 and non-specific protein interactions are minimal (Formalin Cross-linking of Cellular Proteins).
4. Employ a sensitive methodology that permits the identification of small quantities of proteins that specifically bind to cTHY28 (Mass Spectrometric Analysis).

Cell Lines

Previous work demonstrated that elevated levels of cTHY28 are detected in avian lymphoid tissue, with the highest levels being expressed in bursal lymphocytes as compared to thymocytes and splenocytes (1). Since the DT-40 cell line is derived from a bursal lymphoma, this lymphocyte cell line was ideal for studying cellular proteins that interact with cTHY28 (52). The Western Immunoblot analysis (Figure 9, Panel B) clearly confirmed this premise since elevated levels of endogenous cTHY28 expression were readily detected in DT-40 WT cells.

To further enhance the expression of cTHY28 in these cells, a cTHY28/EGFP construct was stably transfected into this lymphocyte cell line (DT-40 N4). Western Immunoblot analysis

confirmed that high levels of cTHY28/EGFP fusion protein were expressed under the influence of the potent Cytomegalovirus Promoter (Figure 9, Panel A). Furthermore, the intense green fluorescence emitted by these cells is indicative of the high level of fusion protein expression in these transfected cells (Figure 2).

Transfection of the DT-40 N4 cells with the cThy28/EGFP construct not only elevated the cellular expression of a cTHY28 fusion protein, it permitted the detection of the subcellular localization of this gene product via the expression of the EGFP marker protein. Comparison of the phase contrast and fluorescent microscopic images clearly demonstrated the nuclear localization of the cTHY28/EGFP fusion protein in the DT-40 N4 cells while expression of EGFP alone was detected throughout the DT-40 V11 cells (Figure 2). This observation is consistent with the nuclear localization motif present in the amino terminus of the cTHY28 protein.

Further analysis of the DT-40 N4 and V11 cell lines indicated that endogenous expression of cTHY28 was diminished in the DT-40 N4 cell lines and elevated in the DT-40 V11 cells as compared to the DT-40 WT cells (Figure 9). This perturbation in cTHY28 expression may reflect a disruption in a cTHY28 feedback mechanism that regulates the cellular levels of this protein (1).

Development of the Co-Immunoprecipitation Assay

In large part, the overall quality of a co-immunoprecipitation assay lies in the specificity of the antibody matrix for the target protein. For this line of investigation, the EGFP component of the cTHY28/EGFP fusion protein was used as a target to co-immunoprecipitate proteins that bind to cTHY28. Antibodies directed against EGFP were generated using a recombinant GFP antigen that was derived from a bacterial expression system (pET28-GFP). The recombinant

GFP protein contained a six amino acid histidine tag that permitted a one-step, metal chelation chromatographic purification of the GFP protein (Figure 3). In turn, the purified GFP protein was used to generate anti-GFP antibodies in chickens. Since the GFP protein (derived from the sea jelly *Aequorea victoria*) represents a phylogenetically distant species from birds, the immunized laying hens developed a robust immune response to this antigen. Relatively large amounts of IgY antibodies (~85 mg per egg) were isolated from the yolks of immune eggs using a simple P.E.G. precipitation technique. DEAE column chromatography was used to further purify this IgY-enriched fraction. The purified IgY antibodies were then covalently linked to a sepharose gel matrix and used in the co-immunoprecipitation assay.

In a similar fashion, the anti-cTHY28 antibodies were generated using a recombinant cThy28 construct that contained a six amino acid histidine tag that permitted the affinity purification of the recombinant protein. The recombinant cTHY28 protein was used as an antigen to immunize rabbits. Anti-cTHY28 antibodies were isolated from immune sera using ammonium sulfate precipitation and DEAE column chromatography(61,62). In turn, these purified N3 antibodies were covalently linked to the affinity matrix.

Formalin cross-linking was employed in the immunoprecipitation procedure to enhance the specificity of identifying putative cTHY28 interacting proteins, as well as stabilize these complexes throughout the isolation procedure. Under the conditions used in this study, formalin-mediated protein-protein cross-linking only occurs when the distance between interacting proteins is approximately 2 A° (63). This stipulation enhances the detection of genuine cTHY28 interacting proteins and minimizes the detection of nonspecific protein interactions. Using the formalin cross-linking procedure also preserves the integrity of interacting protein complexes and thereby enhance the capture of these proteins using the co-immunoprecipitation assay.

Furthermore, formalin cross-linking of interacting proteins with cTHY28 permits the use of stringent assay washing conditions that remove nonspecific proteins attached to the affinity matrix or the cTHY28 protein complex. Surprisingly, putative interacting proteins avidly bind to cTHY28 under these stringent wash conditions in the absence of formalin cross-linking, suggesting a high affinity protein-protein interaction. However as the formalin concentration was increased in the assay, there was a corresponding increase in the detection of putative cTHY28 interacting proteins (Figure 5), indicating that formalin cross-linking enhances the stability of the cTHY28-interacting protein complex.

Co-Immunoprecipitation of Nucleolin and cTHY28

Based upon the analysis of co-immunoprecipitated material from the DT-40 N4 cell lysate, it appears that the cellular function of cTHY28 may be related to the nucleolar protein, nucleolin. The mass spectrometric analysis of the co-immunoprecipitated material clearly indicates that the most prevalent cTHY28 interacting protein is nucleolin. This finding is based upon the number of nucleolin peptides detected in the co-immunoprecipitate, and the relative percentage of the nucleolin amino acid sequence that is covered by these peptides. The cellular function of nucleolin is closely linked to the nucleolus, which has long been considered to be the site of ribosomal biogenesis. Changes in the rate of ribosome production during the cell cycle alter the size of the nucleolus and the distribution of its subcomponents (64,65). Interestingly, this morphological evolution of the nucleolus during the cell cycle has been linked to variations in nucleolar proteins that regulate cell proliferation, cell cycle progression, and pre-rRNA transcriptional processing (64-66). Thus, the cellular function of cTHY28 may be linked to nucleolin since both of these proteins were detected in the co-immunoprecipitate of cell lysates, and both proteins are known to co-localize to the nucleolus.

Nucleolin Function and cTHY28

Nucleolin is the most abundant non-ribosomal protein found in the nucleolus of proliferating cells. This is consistent with its role in meeting the high demand for ribosomal biogenesis and protein biosynthesis in actively dividing cell (67,68). In this capacity, nucleolin is believed to have a variety of functions, including its role as a chaperone for pre-rRNA processing and rDNA transcription (69-75). Likewise, cTHY28 has an elevated level of expression in tissues that have a high rate of cell proliferation, including the bursa of Fabricius, thymus, and testes (1). In addition, nucleolin has been shown to facilitate the translocation of proteins between the nucleolus, nucleus, and cytoplasm (76-79). Since cTHY28 is also found in both the nucleus and nucleolus, it may play a role in facilitating nucleolin dependent protein translocation in these subcellular components. Nucleolin has several other cellular roles that are unrelated to ribosomal biogenesis including: the cellular stress response, mRNA stabilization, chromosomal congression, centrosome duplication, and the internalization of growth factors (75,80-83). Thus, the co-immunoprecipitation of nucleolin and cTHY28 observed in the current studies indicates that cTHY28 may be involved in nucleolin functionality in these cellular processes.

Nucleolin Structural Elements

From a structural perspective, the 100 kDa nucleolin gene product contains four RNA binding domains (RBD 1, 2, 3, 4) which bind to an evolutionary conserved motif located in the 5' external transcribed spacer of the pre-rRNA strand (84). These pre-rRNA transcript motifs are known as nucleolin recognition elements (NREs). The NREs are located in a G-C rich region of the pre-rRNA, which tend to form secondary structural elements of long helices made up of G-C base pairs (85). Nucleolin binds to these NREs as soon as the pre-rRNA is transcribed

and chaperones the folding of the transcript. It is possible that cTHY28 could augment the targeting of nucleolin to its pre-rRNA target (86). Interestingly, there appears to be redundancy in the functionality of the four RBD of nucleolin, since cell viability is not impaired when up to three of these RBD are deleted from the nucleolin gene (74).

Based on all of these known functions of nucleolin, it is no surprise that nucleolin is an essential cellular protein. In fact, a conditional knockout of nucleolin in DT40 cells slows cell proliferation, arrests many cells in G1 phase, and eventually leads to the induction of apoptotic cell death. (74). Furthermore, this knockout alters nucleolar for ultrastructural architecture and impedes rRNA transcription and maturation (74). cTHY28 siRNA does not show a similar lethal phenotype based on RNA interference studies (unpublished data); however, it is possible that a reduction in cTHY28 expression may reduce the efficiency of nucleolin at any of its proposed functions (5).

Co-Immunoprecipitation of Topo I and cTHY28

The second most prevalent cTHY28 interacting protein, based upon mass spectrometric analysis of co-immunoprecipitated cell lysates, was DNA topoisomerase I (topo I). Topo I is a nuclear-localized protein that relaxes supercoiled DNA and thereby facilitates DNA replication and transcription (87,88).

Topo I Function and cTHY28

Mechanistically topo I accomplishes this relaxation by binding to DNA and cleaving one strand at the 3' terminus to form a transient enzyme-DNA complex. This step is followed by the relaxation of the supercoil DNA, ligation of the nicked DNA strand, and release of topo I from the DNA strand (89,90). Thus, topo I enhances transcription of genes that are heavily transcribed, such as RNA polymerase I and II, by preferentially binding to DNA targets within

these genes to ease the torsional stress due to elongation and relieve the supercoiled tension that develops in the DNA strand during transcription (87,88,91-94).

Inhibition of topo I has been shown to block transcription and replication events; however, in yeast mutants that lack topo I, nearly normal growth was observed, indicating that other topoisomerases may compensate for the lack of topo I (94-97). However, these mutants demonstrated an increased incidence of aberrant rDNA recombination, indicating that topo I plays a critical role in maintaining the integrity of the rDNA loci (98).

Topo I activity is regulated through the phosphorylation/dephosphorylation of critical serine residues in the protein. Phosphorylation of serine residues enhances activity of topo I, while dephosphorylation by alkaline phosphatase decreases its activity (98-100). Caesin-kinase II-like kinase and protein kinase C have been shown to activate topo I (99,101). Interestingly, cTHY28 has putative caesin-kinase II and protein kinase C phosphorylation sites in its amino acid sequence that may play a similar role in regulating functional activity.

Topo I nuclear function appears to be associated with the nucleolus (102-105). Topo I has been shown to associate with two nucleolar proteins, RNA polymerase I and nucleolin (106,107). More specifically, the 166-210 amino acid region in human topo I has been identified as the protein-protein binding region for nucleolin, and topo I (106). Since deletion of the nucleolin binding site does not impair topo I's ability to relax supercoiled plasmid DNA in yeast, it is hypothesized that nucleolin may help target topo I to transcription sites. This hypothesis is supported by prior studies which demonstrate interactions of topo I with other transcription proteins such as RNA polymerase I, TATA-binding protein, and high mobility group proteins (106-109). A second hypotheses suggests that topo I function is enhanced by nucleolin-dependent transport of topo I between the nucleolar, nuclear, and cytoplasmic compartment of

the cell (110). Since cTHY28 may interact with both nucleolin and topo I, it may enhance the translocation of topo I between the nuclear and nucleolar compartments, or enhance targeting of topo I to its transcriptional targets.

Co-Immunoprecipitation of Elongation Factor-2 and cTHY28

The third most prevalent cTHY28 interacting protein, based upon mass spectrometric analysis of co-immunoprecipitated cell lysates, was elongation factor-2 (EF-2). EF-2 is a 93 kDa GTPase protein, that is involved in the elongation process of translation (111). More specifically, it is involved in the translocation of the peptide-tRNA complex from the A-site to the P-site of the 80S ribosome (111). EF-2 is primarily localized in the cytoplasmic compartment of the cell (112-114). Since EF-2 is a cytoplasmic protein, compared to the nuclear/nucleolar localization of nucleolin, topo I, and cTHY28, interaction between EF-2 and cTHY28 may be a consequence of the over-expression of the cTHY28/EGFP protein in the DT-40 cells. The association of EF-2 and cTHY28 may reflect a transient interaction between these two proteins that occurs during the elevated expression of the cTHY28/EGFP fusion protein. This theory is supported by the fact that EF-2 expression is elevated in cancer cells, which overexpress specific cellular proteins (115).

Interestingly, cTHY28, topo I, and nucleolin share several characteristics that support a model for protein-protein interaction. All three proteins are putative targets for phosphorylation by CKII or CKII-like kinases, and cTHY28, more over topo I are putative targets for phosphorylation by protein kinase C, as well. All three proteins co-localize to the nucleus and the nucleolus. Thus, cTHY28 may form a protein complex with topo I and nucleolin that is involved in nuclear functions related to transcription, DNA replication, and rRNA processing. Furthermore, this complex appears to be a weak, or a transitional association of these proteins

since it was necessary to employ a formalin cross-linking technique to stabilize the protein complex before it could be co-immunoprecipitated. Electrophoretic separation of the co-immunoprecipitate and subsequent mass spectrometric analysis revealed that both topo I and nucleolin were identified in the gel band that migrated at 120 kDa as shown in Figure 10. This observation suggests that the protein complex disassociates after being co-immunoprecipitated during the antibody matrix elution step, or during the SDS-PAGE step. Due to the potential disassociation of the protein complex at either of these analytical steps, it is unknown whether the cTHY28 forms a complex with both topo I and nucleolin at the same time, or if cTHY28 interacts independently with topo I and nucleolin. Further research into manipulating, not only cellular levels of cTHY28, but manipulating levels of nucleolin and topo I, in conjunction with cTHY28 levels, could help determine cTHY28's specific role in this putative complex with topo I and nucleolin.

In the final analysis, the cellular function of cTHY28 remains unknown. Based on previous work, it was assumed that cTHY28 was involved in the apoptotic cell death pathway. However, the data presented here in shows evidence that cTHY28 may be interacting in the ribosomal RNA biosynthetic pathway. Thus, it is conceivable that cTHY28 may act exclusively or directly in this role. Nevertheless, it is also possible that cTHY28 may act as an apoptotic mediator by its interactions with ribosomal RNA biosynthesis pathway.

References

1. Compton, M., Thomson, J. M., and Icard, A. (2001) *Apoptosis* **6**, 299-314
2. Miyaji, H., Yoshimoto, T., Asakura, H., Komachi, A., Kamiya, S., Takasaki, M., and Mizuguchi, J. (2002) *Gene* **297**, 189-196
3. Jiang, X. Z., Toyota, H., Yoshimoto, T., Takada, E., Asakura, H., and Mizuguchi, J. (2003) *Apoptosis* **8**, 509-519
4. Jiang, X., Toyota, H., Takada, E., Yoshimoto, T., Kitamura, T., Yamada, J., and Mizuguchi, J. (2003) *Tissue and Cell* **35**, 471-478
5. Purdee, M. L. (2006) *Analysis of hThy28 expression in HeLa cells.* M.S. Thesis, University of Georgia, Athens
6. Fernandez-Arias, A., Martinez, S., and Rodriguez, J. (1997) *J. Virol.* **71**, 8014-8018
7. Rodriguez-Lecompte, J. C., Nino-Fong, R., Lopez, A., Frederick Markham, R. J., and Kibenge, F. S. (2005) *Comp Immunol Microbiol Infect Dis* **28**, 321-337
8. Ruby, T., Whittaker, C., Withers, D. R., Chelbi-Alix, M. K., Morin, V., Oudin, A., Young, J. R., and Zoorob, R. (2006) *J. Virol.* **80**, 9207-9216
9. Vasconcelos, A. C., and Lam, K. M. (1994) *Journal of General Virology* **75**, 1803-1806
10. Vasconcelos, A. C., and Lam, K. M. (1995) *J Comp Pathol* **112**, 327-338
11. Ideker, T., Thorsson, V., Ranish, J. A., Christmas, R., Buhler, J., Eng, J. K., Bumgarner, R., Goodlett, D. R., Aebersold, R., and Hood, L. (2001) *Science* **292**, 929-934
12. Beeckmans, S. (1999) *Methods* **19**, 278-305
13. Mowbray, J., and Moses, V. (1976) *European Journal of Biochemistry* **66**, 25-36
14. Porpaczy, Z., S¸megi, B. z., and Alkonyi, I. n. (1983) *Biochimica et Biophysica Acta (BBA) - Protein Structure and Molecular Enzymology* **749**, 172-179
15. Kellogg, D. R., and Moazed, D. (2002) Protein- and immunoaffinity purification of multiprotein complexes. in *Methods in Enzymology* (Christine Guthrie, G. R. F. ed.), Academic Press. pp 172-183
16. Altman, R., and Kellogg, D. (1997) *The Journal of Cell Biology* **138**, 119-130
17. Aroian, R. V., Field, C., Pruliere, G., Kenyon, C., and Alberts, B. M. (1997) *EMBO J* **16**, 1541-1549
18. Carroll, C. W., Altman, R., Schieltz, D., Yates, J. R., and Kellogg, D. (1998) *The Journal of Cell Biology* **143**, 709-717
19. Kellogg, D. R., Field, C. M., and Alberts, B. M. (1989) *The Journal of Cell Biology* **109**, 2977-2991
20. Kellogg, D. R., Kikuchi, A., Fujii-Nakata, T., Turck, C. W., and Murray, A. W. (1995) *The Journal of Cell Biology* **130**, 661-673
21. Miller, K. G., and Alberts, B. M. (1989) *Proceedings of the National Academy of Sciences* **86**, 4808-4812
22. Moazed, D., and Johnson, A. D. (1996) *Cell* **86**, 667-677
23. Straight, A. F., Shou, W., Dowd, G. J., Turck, C. W., Deshaies, R. J., Johnson, A. D., and Moazed, D. (1999) *Cell* **97**, 245-256

24. Thompson, C. M., Koleske, A. J., Chao, D. M., and Young, R. A. (1993) *Cell* **73**, 1361-1375
25. Rhemrev-Boom, M. M., Yates, M., Rudolph, M., and Raedts, M. (2001) *Journal of Pharmaceutical and Biomedical Analysis* **24**, 825-833
26. Cuatrecasas, P., Wilchek, M., and Anfinsen, C. B. (1968) *Proc Natl Acad Sci U S A* **61**, 636-643
27. HjertÈn, S., and Mosbach, R. (1962) *Analytical Biochemistry* **3**, 109-118
28. Hofstee, B. H. J. (1975) *Biochemical and Biophysical Research Communications* **63**, 618-624
29. Burgess, R. R., and Thompson, N. E. (2002) *Current Opinion in Biotechnology* **13**, 304-308
30. Moresco, J. J., Carvalho, P. C., and Yates, J. R. (2010) *Journal of Proteomics* **73**, 2198-2204
31. Shimomura, O., Johnson, F. H., and Saiga, Y. (1962) *Journal of Cellular and Comparative Physiology* **59**, 223-239
32. Zhang, L., Ding, L., Cheung, T. H., Dong, M.-Q., Chen, J., Sewell, A. K., Liu, X., Yates Iii, J. R., and Han, M. (2007) *Molecular Cell* **28**, 598-613
33. Gavin, A.-C., Bosche, M., Krause, R., Grandi, P., Marzioch, M., Bauer, A., Schultz, J., Rick, J. M., Michon, A.-M., Cruciat, C.-M., Remor, M., Hofert, C., Schelder, M., Brajenovic, M., Ruffner, H., Merino, A., Klein, K., Hudak, M., Dickson, D., Rudi, T., Gnau, V., Bauch, A., Bastuck, S., Huhse, B., Leutwein, C., Heurtier, M.-A., Copley, R. R., Edelmann, A., Querfurth, E., Rybin, V., Drewes, G., Raida, M., Bouwmeester, T., Bork, P., Seraphin, B., Kuster, B., Neubauer, G., and Superti-Furga, G. (2002) *Nature* **415**, 141-147
34. Ho, Y., Gruhler, A., Heilbut, A., Bader, G. D., Moore, L., Adams, S.-L., Millar, A., Taylor, P., Bennett, K., Boutilier, K., Yang, L., Wolting, C., Donaldson, I., Schandorff, S., Shewnarane, J., Vo, M., Taggart, J., Goudreault, M., Muskat, B., Alfarano, C., Dewar, D., Lin, Z., Michalickova, K., Willems, A. R., Sassi, H., Nielsen, P. A., Rasmussen, K. J., Andersen, J. R., Johansen, L. E., Hansen, L. H., Jespersen, H., Podtelejnikov, A., Nielsen, E., Crawford, J., Poulsen, V., Sorensen, B. D., Matthiesen, J., Hendrickson, R. C., Gleeson, F., Pawson, T., Moran, M. F., Durocher, D., Mann, M., Hogue, C. W. V., Figeys, D., and Tyers, M. (2002) *Nature* **415**, 180-183
35. Sali, A., Glaeser, R., Earnest, T., and Baumeister, W. (2003) *Nature* **422**, 216-225
36. Fancy, D. A. (2000) *Current Opinion in Chemical Biology* **4**, 28-33
37. Orlando, V. (2000) *Trends in Biochemical Sciences* **25**, 99-104
38. Orlando, V., Strutt, H., and Paro, R. (1997) *Methods* **11**, 205-214
39. Vasilescu, J., Guo, X., and Kast, J. (2004) *Proteomics* **4**, 3845-3854
40. Fragoso, G., and Hager, G. L. (1997) *Methods* **11**, 246-252
41. Hall, D. B., and Struhl, K. (2002) *Journal of Biological Chemistry* **277**, 46043-46050
42. Jackson, V. (1999) *Methods* **17**, 125-139
43. Edman, P. (1949) *Arch Biochem* **22**, 475
44. Bauer, A., and Kuster, B. (2003) *European Journal of Biochemistry* **270**, 570-578
45. Monteoliva, L., and Albar, J. P. (2004) *Briefings in Functional Genomics & Proteomics* **3**, 220-239
46. Henzel, W. J., Billeci, T. M., Stults, J. T., Wong, S. C., Grimley, C., and Watanabe, C. (1993) *Proceedings of the National Academy of Sciences* **90**, 5011-5015

47. Yates, J. R. (2004) *Annual Review of Biophysics and Biomolecular Structure* **33**, 297-316
48. Felitsyn, N., Peschke, M., and Kebarle, P. (2002) *International Journal of Mass Spectrometry* **219**, 39-62
49. Hunt, D. F., Yates, J. R., Shabanowitz, J., Winston, S., and Hauer, C. R. (1986) *Proceedings of the National Academy of Sciences* **83**, 6233-6237
50. Eng, J. K., McCormack, A. L., and Yates Iii, J. R. (1994) *Journal of the American Society for Mass Spectrometry* **5**, 976-989
51. Perkins, D. N., Pappin, D. J., Creasy, D. M., and Cottrell, J. S. (1999) *Electrophoresis* **20**, 3551-3567
52. Baba, T. W., Giroir, B. P., and Humphries, E. H. (1985) *Virology* **144**, 139-151
53. Cormack, B. P., Valdivia, R. H., and Falkow, S. (1996) *Gene* **173**, 33-38
54. Jensenius, J. C., Andersen, I., Hau, J., Crone, M., and Koch, C. (1981) *Journal of Immunological Methods* **46**, 63-68
55. Towbin, H., Staehelin, T., and Gordon, J. (1992) *Biotechnology (Reading, Mass.)* **24**, 145-149
56. Espino, J. J., Gutierrez-Sanchez, G., Brito, N., Shah, P., Orlando, R., and Gonzalez, C. (2010) *Proteomics* **10**, 3020-3034
57. Shah, P., Gutierrez-Sanchez, G., Orlando, R., and Bergmann, C. (2009) *Proteomics* **9**, 3126-3135
58. Pedrioli, P. G. A., Eng, J. K., Hubley, R., Vogelzang, M., Deutsch, E. W., Raught, B., Pratt, B., Nilsson, E., Angeletti, R. H., Apweiler, R., Cheung, K., Costello, C. E., Hermjakob, H., Huang, S., Julian, R. K., Kapp, E., McComb, M. E., Oliver, S. G., Omenn, G., Paton, N. W., Simpson, R., Smith, R., Taylor, C. F., Zhu, W. M., and Aebersold, R. (2004) *Nat. Biotechnol.* **22**, 1459-1466
59. Weatherly, D. B., Atwood, J. A., Minning, T. A., Cavola, C., Tarleton, R. L., and Orlando, R. (2005) *Mol. Cell. Proteomics* **4**, 762-772
60. Link, A. J., Eng, J., Schieltz, D. M., Carmack, E., Mize, G. J., Morris, D. R., Garvik, B. M., and Yates, J. R., 3rd. (1999) *Nat Biotechnol* **17**, 676-682
61. Liddell, J. E. (2001) Antibody Purification by Ammonium Sulfate Precipitation. in *eLS*, John Wiley & Sons, Ltd. pp
62. Corthier, G., Boschetti, E., and Charley-Poulain, J. (1984) *Journal of Immunological Methods* **66**, 75-79
63. Orlando, V., and Paro, R. (1993) *Cell* **75**, 1187-1198
64. Cerdido, A., and Medina, F. J. (1995) *Chromosoma* **103**, 625-634
65. Klein, J., and Grummt, I. (1999) *Proceedings of the National Academy of Sciences of the United States of America* **96**, 6096-6101
66. Medina, F. J., Cerdido, A., and de Carcer, G. (2000) *Eur. J. Histochem.* **44**, 117-131
67. Bugler, B., Caizerguesferrer, M., Bouche, G., Bourbon, H., and Amalric, F. (1982) *European Journal of Biochemistry* **128**, 475-480
68. Busch H, B. N., Rao MRS, Choi YC. (1978) *The Cell Nucleus* **5**, 416-168
69. Alvarez, M., Quezada, C., Navarro, C., Molina, A., Bouvet, P., Krauskopf, M., and Vera, M. I. (2003) *Biochemical and Biophysical Research Communications* **301**, 152-158
70. Medina, F. J., Gonzalez-Camacho, F., Manzano, A. I., Manrique, A., and Herranz, R. (2010) *J. Appl. Biomed.* **8**, 141-150
71. Rickards, B., Flint, S. J., Cole, M. D., and LeRoy, G. (2007) *Mol. Cell. Biol.* **27**, 937-948

72. Roger, B., Moisand, A., Amalric, F., and Bouvet, P. (2002) *Journal of Biological Chemistry* **277**, 10209-10219
73. Roger, B., Moisand, A., Amalric, F., and Bouvet, P. (2003) *Chromosoma* **111**, 399-407
74. Storck, S. b., Thiry, M., and Bouvet, P. (2009) *Biology of the Cell* **101**, 153-167
75. Ugrinova, I., Monier, K., Ivaldi, C., Thiry, M., Storck, S., Mongelard, F., and Bouvet, P. (2007) *BMC Mol. Biol.* **8**
76. Borer, R. A., Lehner, C. F., Eppenberger, H. M., and Nigg, E. A. (1989) *Cell* **56**, 379-390
77. Erard, M. S., Belenguer, P., Caizerguesferrer, M., Pantaloni, A., and Amalric, F. (1988) *European Journal of Biochemistry* **175**, 525-530
78. Herrera, A. H., and Olson, M. O. J. (1986) *Biochemistry* **25**, 6258-6264
79. Srivastava, M., Fleming, P. J., Pollard, H. B., and Burns, A. L. (1989) *FEBS Lett.* **250**, 99-105
80. De, A. Y., Donahue, S. L., Tabah, A., Castro, N. E., Mraz, N., Cruise, J. L., and Campbell, C. (2006) *Biochemical and Biophysical Research Communications* **344**, 206-213
81. Ma, N., Matsunaga, S., Takata, H., Ono-Maniwa, R., Uchiyama, S., and Fukui, K. (2007) *J. Cell Sci.* **120**, 2091-2105
82. Shibata, Y., Muramatsu, T., Hirai, M., Inui, T., Kimura, T., Saito, H., McCormick, L. M., Bu, G. J., and Kadomatsu, K. (2002) *Mol. Cell. Biol.* **22**, 6788-6796
83. Takagi, M., Absalon, M. J., McLure, K. G., and Kastan, M. B. (2005) *Cell* **123**, 49-63
84. Ginisty, H., Serin, G., Ghisolfi-Nieto, L., Roger, B., Libante, V., Amalric, F., and Bouvet, P. (2000) *Journal of Biological Chemistry* **275**, 18845-18850
85. Renalier, M. H., Mazan, S., Joseph, N., Michot, B., and Bachellerie, J. P. (1989) *FEBS Lett.* **249**, 279-284
86. Allain, F. H., Bouvet, P., Dieckmann, T., and Feigon, J. (2000) *EMBO J* **19**, 6870-6881
87. Liu, L. F., and Wang, J. C. (1987) *Proceedings of the National Academy of Sciences of the United States of America* **84**, 7024-7027
88. Wang, J. C., and Lynch, A. S. (1993) *Current Opinion in Genetics & Development* **3**, 764-768
89. Reguera, R. M., Redondo, C. M., Gutierrez de Prado, R., Pérez-Pertejo, Y., and Balaña-Fouce, R. *Biochimica et Biophysica Acta (BBA) - Gene Structure and Expression* **1759**, 117-131
90. Stewart, L., Redinbo, M. R., Qiu, X. Y., Hol, W. G. J., and Champoux, J. J. (1998) *Science* **279**, 1534-1541
91. Gilmour, D. S., Pflugfelder, G., Wang, J. C., and Lis, J. T. (1986) *Cell* **44**, 401-407
92. Kroeger, P. E., and Rowe, T. C. (1992) *Biochemistry* **31**, 2492-2501
93. Wang, J. C. (1985) *Annu. Rev. Biochem.* **54**, 665-697
94. Zhang, H., Wang, J. C., and Liu, L. F. (1988) *Proceedings of the National Academy of Sciences of the United States of America* **85**, 1060-1064
95. Liu, L. F. (1989) *Annu. Rev. Biochem.* **58**, 351-375
96. Wang, J. C. (1991) *Journal of Biological Chemistry* **266**, 6659-6662
97. Wu, H. Y., Shyy, S., Wang, J. C., and Liu, L. F. (1988) *Cell* **53**, 433-440
98. Christman, M. F., Dietrich, F. S., and Fink, G. R. (1988) *Cell* **55**, 413-425
99. Pommier, Y., Kerrigan, D., Hartman, K. D., and Glazer, R. I. (1990) *Journal of Biological Chemistry* **265**, 9418-9422
100. Samuels, D. S., Shimizu, Y., and Shimizu, N. (1989) *FEBS Lett.* **259**, 57-60

101. Turman, M. A., and Douvas, A. (1993) *Biochemical Medicine and Metabolic Biology* **50**, 210-225
102. Maul, G. G., French, B. T., Vanvenrooij, W. J., and Jimenez, S. A. (1986) *Proceedings of the National Academy of Sciences of the United States of America* **83**, 5145-5149
103. Muller, M. T., Pfund, W. P., Mehta, V. B., and Trask, D. K. (1985) *Embo J.* **4**, 1237-1243
104. Negri, C., Chiesa, R., Cerino, A., Bestagno, M., Sala, C., Zini, N., Maraldi, N. M., and Ricotti, G. (1992) *Exp. Cell Res.* **200**, 452-459
105. Oddou, P., Schmidt, U., Knippers, R., and Richter, A. (1988) *European Journal of Biochemistry* **177**, 523-529
106. Bharti, A. K., Olson, M. O. J., Kufe, D. W., and Rubin, E. H. (1996) *Journal of Biological Chemistry* **271**, 1993-1997
107. Rose, K. M., Szopa, J., Han, F. S., Cheng, Y. C., Richter, A., and Scheer, U. (1988) *Chromosoma* **96**, 411-416
108. Javaherian, K., and Liu, L. F. (1983) *Nucleic Acids Res.* **11**, 461-472
109. Merino, A., Madden, K. R., Lane, W. S., Champoux, J. J., and Reinberg, D. (1993) *Nature* **365**, 227-232
110. Alsner, J., Svejstrup, J. Q., Kjeldsen, E., Sorensen, B. S., and Westergaard, O. (1992) *Journal of Biological Chemistry* **267**, 12408-12411
111. Jorgensen, R., Merrill, A. R., and Andersen, G. R. (2006) *Biochem Soc Trans* **34**, 1-6
112. Bektas, M., Nurten, R., Gurel, Z., Sayers, Z., and Bermek, E. (1994) *FEBS Lett.* **356**, 89-93
113. Bektas, M., Nurten, R., Sayers, Z., and Bermek, E. (1998) *European Journal of Biochemistry* **256**, 142-147
114. Shestakova, E. A., Motuz, L. P., Minin, A. A., Gelfand, V. I., and Gavrilova, L. P. (1991) *Cell Biology International Reports* **15**, 75-84
115. Nakamura, J., Aoyagi, S., Nanchi, I., Nakatsuka, S. I., Hirata, E., Shibata, S., Fukuda, M., Yamamoto, Y., Fukuda, I., Tatsumi, N., Ueda, T., Fujiki, F., Nomura, M., Nishida, S., Shirakata, T., Hosen, N., Tsuboi, A., Oka, Y., Nezu, R., Mori, M., Doki, Y., Aozasa, K., Sugiyama, H., and Oji, Y. (2009) *Int. J. Oncol.* **34**, 1181-1189